Investigation of Variations in Corrosion Potential in Mechanically Stabilized Earth Backfill Due to Migration of Fines

By

Chase Vincent Breckwoldt

B.Sc., the University of Kansas, 2017

Submitted to the graduate degree program in the Department of Civil, Environmental, and Architectural Engineering and the Graduate Faculty of the University of Kansas in partial fulfillment of the requirements for the degree of Master of Science.

_____

Chair: Dr. Robert Parsons

_____

Dr. Jie Han

_____

Dr. Matt O'Reilly

Date Defended: 1 May 2019

The thesis committee for Chase Vincent Breckwoldt certifies that

this is the approved version of the following thesis:

Investigation of Variations in Corrosion Potential in Mechanically Stabilized Earth Backfill Due to Migration of Fines

_____

Chair: Dr. Robert Parsons

Date Approved: 1 May 2019

ABSTRACT

Departments of transportation have constructed thousands of mechanically stabilized earth (MSE) walls to support bridge abutments in highway projects and for other applications. These MSE walls often include metal strips or grids as reinforcement, typically galvanized steel strips within granular backfill meeting Federal Highway Administration (FHWA) and American Association of State Highway and Transportation Officials (AASHTO) standards. Utilization of steel strips or grids creates a stronger composite material; however, minerals within the backfill or salts applied at the surface can create a corrosive environment. Excessive corrosion can lead to distresses or premature failure of MSE structures.

Corrosion may increase when cycles of water from precipitation promote migration of fines through the granular backfill. Migrating fines have the potential to accumulate at the base of the reinforced fill and clog drainage and retain water, which could accelerate the corrosion process.

This study evaluated the potential for accelerated corrosion due to the accumulation of fines with water. Aggregate approved for use in MSE structures was placed in a test column with internal dimensions of 183 by 30 by 30 cm and flowing water through it. The grain size distribution was measured at different elevations within the column and the resistivity of the aggregate, which is correlated with corrosion rate, was also evaluated at a series of elevations within the column after passing water through the column. Results from the testing were compared with resistivity results from a test box consistent with current Kansas Department of Transportation (KDOT) use. All aggregates tested had a drained resistivity that was above the 3000 or 5000-ohm centimeter (ohm-cm) minimum.

The results of this study show that migration of fines occur in KDOT aggregates, and that this migration can cause measurable changes in the grain size distribution, water content, and resistivity of the soil column. In addition, as the number of saturated and drained cycles increases for each material, the resistivity increases. The current KDOT specification limiting the amount of material passing the No. 200 sieve is beneficial in that it limits the fines available for migration. Additional constraints within the specification could further limit the potential for suffusion.

ACKNOWLEDGMENTS

The authors would like to thank Mr. Luke Metheny and Mr. Bryan Pope and the Kansas Department of Transportation (KDOT) for providing the financial and logistical support for the research described in this thesis; the University of Kansas for providing support for this research; Mr. Kent Dye and Mr. David Woody of the University of Kansas for their assistance in fabricating the test box; and Mr. Jim Brennan of KDOT and Mrs. Tanya Walkenbach for their assistance with data collection.

TABLE OF CONTENTS

LIST OF TABLES

LIST OF FIGURES

This page intentionally left blank.

CHAPTER 1: INTRODUCTION

Departments of transportation and other organizations have constructed many mechanically stabilized earth (MSE) walls to support bridge abutments for highway projects and other applications. MSE walls often include metal strips or grids as reinforcement, typically galvanized steel strips within granular backfill meeting Federal Highway Administration (FHWA) and American Association of State Highway and Transportation Officials (AASHTO) standards. This reinforcement is critical to maintaining the stability of the wall. A common design used by the Kansas Department of Transportation (KDOT) and many other organizations includes using concrete panels for aesthetics, to prevent the soil from raveling at the wall face, and to provide a connection surface for reinforcing elements. Utilization of steel strips or grids creates a strong reinforced backfill material; however, minerals within the backfill or salts applied at the surface can create a corrosive environment, potentially resulting in corrosion of the steel reinforcement. Excessive corrosion can lead to distresses or premature failure of MSE structures. Aggregates that are candidates for use as backfill are commonly tested using resistivity as a proxy for potential of corrosion. Aggregates with low resistivity are more corrosive and may be subject to additional testing or rejected on this basis.

1.1 Effect of Resistivity on Corrosion Potential: Electrical Resistivity

Soil resistivity is defined as the inverse of conductivity and has units of ohm-centimeters (ohm-cm) or ohm meters (ohm-m). Electrolytic behavior of soils is an indirect measurement of soluble salt content, and one factor controlling soil resistivity is the concentration of dissolved anions resulting in a strong influence on macro-corrosion cells that may form on buried metal (Elias et al., 2009). To counter the effects of corrosion, sacrificial thickness requirements for galvanized reinforcement have been established for metal reinforcement as a function of the

corrosivity of the environment, to ensure satisfactory performance throughout the design life. The corrosivity of placed backfill is a function of electrical resistivity, pH, sulfates, chlorides and organics concentrations. Elias et al. (2009) found that as soil porosity and salinity increase, the resistivity of the soil decreases. In addition, Elias et al. (2009) found that the most common form of corrosion within soil for a moisture content ranging from 25 to 40% is pitting.

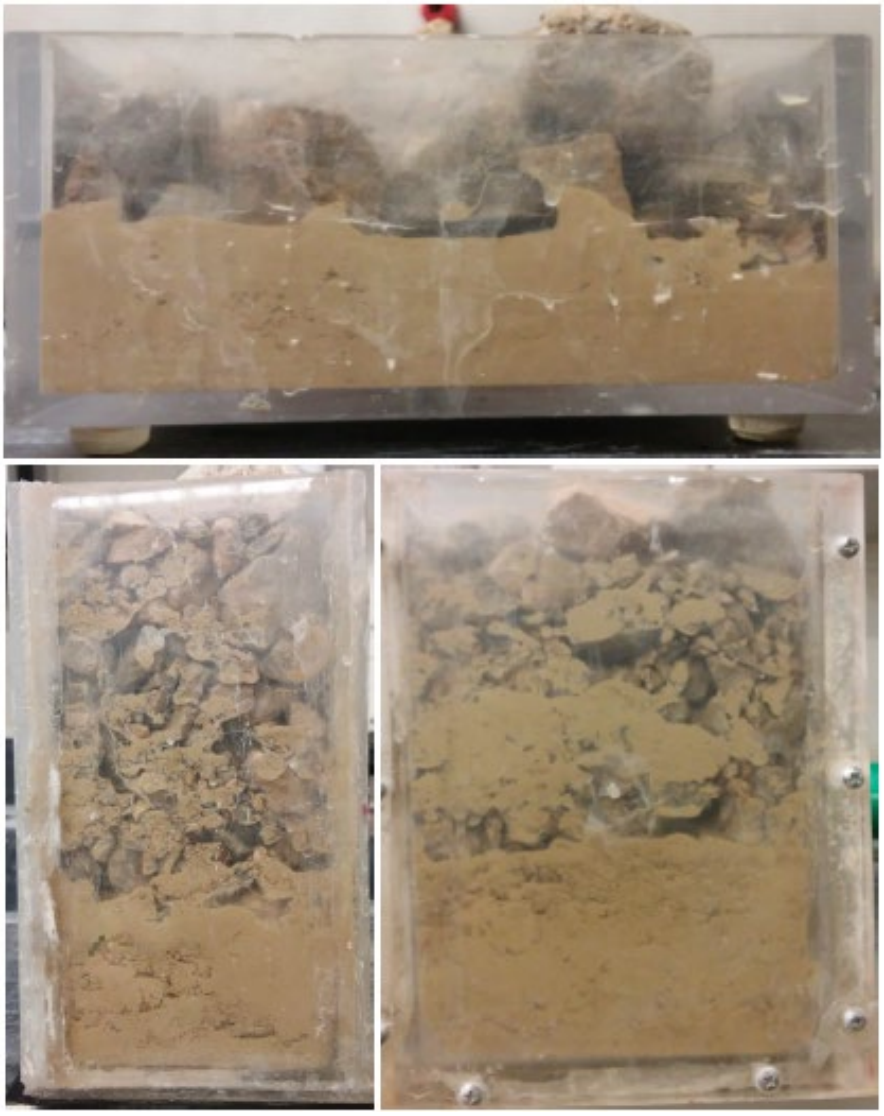

Figure 1.1. Ridgeview ASTM CXXX-XX Sample after Soaking and Draining Cycles: AASHTO Box (top), Small Box (left), and Large Box (right) (Brady et al., 2016).

The backfills used in MSE walls constructed by KDOT consist primarily of river sands and limestone aggregate. Since fines and various ionic concentrations are still present within the sands and aggregate backfill, the concern for corrosion is warranted. Departments of transportation, including KDOT, commonly test aggregates for resistivity as a proxy for corrosion. This testing assumes that aggregate backfills are a homogeneous mass. During previous research at the University of Kansas (KU), Brady et al. (2016) observed that at least one aggregate source approved by KDOT demonstrated significant particle migration within the sample, resulting in backfill aggregate with a high percent of fines at the bottom of the sample. Figure 1.1 shows the migration of fines within a test box as documented by Brady et al. (2016). This portion of the sample greatly inhibited drainage and caused retention of a large amount of water. When this phenomenon was observed, it was recognized that if inhibited drainage and water retention occurred in a large fill a layer of aggregate with a high percentage of fines could encase the lower levels of metallic reinforcement. This layer with concentrated fines and a higher water content could lead to much faster rates of corrosion. It was therefore determined that investigation of the potential for fines migration within KDOT aggregates should be investigated.

As mentioned above, migrating fines within MSE walls have the potential to accumulate at the base of the reinforced fill which could clog drainage, retain water and lead to an accelerated corrosion process. In addition, fines within granular backfill may disproportionately carry the electrochemical constituents that contribute to the acceleration of corrosion of metal reinforcement. The scope of this research addresses changes in electrical resistivity due to the migration of fines by testing five aggregates meeting the specifications in KDOT Manual Section 1107, Aggregates for Backfill, within a 30.5-by-30.5-by-182.9-cm box (length-width-height). Cycles of water promoting fine migration (suffusion) downward through the granular backfill were

added to model cycles of precipitation in the field. The grain size distribution was measured at different elevations within the column, and the resistivity of the aggregate, which is correlated with corrosion rate, was estimated at a series of elevations within the test column after saturated and drained cycles.

The format of the remainder of this thesis is as follows: Chapter 2 contains a review of the relevant literature; Chapter 3 contains a description of the scope of work of this study, procedures followed, and equipment used; Chapter 4 contains the results of testing and subsequent analysis; and Chapter 5 contains the conclusions and recommendations developed from this study.

CHAPTER 2: LITERATURE REVIEW

The potential for corrosion of metallic reinforcement within aggregate backfill is considered when designing retaining walls and other geotechnical structures. The technique of implementing metallic reinforcement became common practice since the 1970s. Aggregates used in MSE walls and other applications within Kansas are typically limestone aggregates larger than half an inch. River sands are also commonly used. KDOT has set out standards in Section 1107, Aggregates for Backfill, to regulate grain size distribution, pH levels, ion concentrations, organics, soundness, and wear of aggregates. In addition, because the potential for corrosion of an aggregate is correlated with its resistivity, resistivity specifications for backfill aggregate are included in MSE wall design where corrosion is a potential concern. Resistivity is normally assumed to be consistent throughout the backfill behind an MSE structure; however, previous work at KU has shown that migration of fines can change resistivity and potential for corrosion and is potentially cause for concern (Brady et al., 2016). The objective of this research was to measure resistivity changes within backfill due to the migration of fines, with particular focus on the increase of potential for corrosion as fines migrate downward, concentrating at the bottom of reinforced structures.

2.1 MSE WALLS

The use of metallic reinforcement allows engineers to design stronger, taller, and more stable MSE walls to support larger loads. Layers of metallic reinforcement placed within compacted aggregate create a strong and stable reinforced material. The reinforcement consists of galvanized steel rebar or strips of different sizes, dependent on expected design loads. However, failure to accurately test the backfill's electrochemical properties can lead to premature failure of

metallic reinforcement: migration and concentration of fines can accelerate corrosion by creating a more corrosive environment at the base of the fill.

The design life of a MSE wall is a consideration when specifying the size of the metallic reinforcement being used. In addition to the size of bar or strip thickness, the life of the wall must be considered when determining the amount of sacrificial steel needed to support the design load within an appropriate range for a specified factor of safety.

2.2 Internal Erosion via Suffusion

Suffusion processes are characterized by the progressive and diffusive migration of fine particles over time. Suffusion is the detachment, transport, and re-deposition of fine particles in the pore space between coarser particles (Sibille et al., 2014). Suffusion is also defined as the internal instability within an aggregate or soil matrix. It corresponds to the process of detachment and transport of fines within the porous aggregate. This internal instability is a result of the inability of the backfill aggregate to act as a geo-filter to prevent the loss of its own small particles (Kenney and Lau, 1985). Wan and Fell (2008) describe the conditions for suffusion thus; "the soil possesses a specific structure in which a coarse fraction is formed, loose particles fill voids formed by the coarser fraction, finer soil particles must be smaller than the constrictions of the coarser fraction, and the flow is capable of carrying the loose particles through the voids." In MSE walls, water flow and gravity act as the primary forces for carrying fine particles through the voids of the coarse aggregate. In addition, due to the migration of fines, the soil permeability at the base of the fill is decreased, as many of the eroded particles have been transported to the bottom layer during the migration process, causing clogging of constrictions (Chang and Zhang, 2011). As a result of suffusion, two stages of migration can occur. The first is the migration of fines slowly from the upper fraction toward the bottom fraction. Second, a washing out of fines may occur, potentially

inducing large settlement and an increase of hydraulic conductivity in highly layered aggregate (Sibille et al., 2014). The susceptibility to suffusion is based on a hydraulic gradient, hydraulic shear stress, and pore velocity, which is governed by the geometry of the porous network and the physicochemical interactions between the pore fluid and solid grains on the aggregate (Marot et al., 2016). In addition, the movement of small particles is dependent on the density of the material, grain size distribution, and the severity of seepage and vibration forces (Kenney and Lau, 1985).

Marot et al. (2012) tested three coarse-grained sands with 10% kaolin as the fine fraction and found that suffusion resistance increases as the angularity of sand particles is increased. This is more applicable to sand, because in an aggregate containing material of larger size the void space may be more important than the angularity of the coarse particles within the aggregate. Further research on this topic within a larger permeability apparatus is warranted.

2.3 Corrosion and Degradation of the Aggregate Reinforcement

Corrosion is fundamentally a return of metals to their native state as oxides and salts. Corrosion is the deterioration or dissolution of metal by chemical or electrochemical reactions within the metal's environment (Elias et al., 2009). When soils are evenly compacted and resistivity measurements are taken, the primary location of concern about excessive corrosion is at the face and base of wall structures, based on DOT reports. A study by Romanoff (1957), based on years of data collection, reported that the first few years of burial have the highest rates of corrosion. Corrosion rates are directly linked to the electrochemical properties of the compacted aggregate (Thapalia et al., 2011). The approach for designing an MSE wall against corrosion includes estimating the expected loss of both zinc and steel during the design life, and then adding sufficient sacrificial steel to the reinforcement cross section to ensure the end of design life will be reached for the allowable stress conditions (Elias et al., 2009). To minimize the sacrificial

thickness, standards directing the selection of a fill with appropriate electrochemical properties have been developed. Arciniega (2017) confirmed that coarse aggregates have minimum resistivity at 100% saturation for the aggregate. In addition, Edlerback and Beske (2014) confirmed an inverse relationship between moisture content and aggregate resistivity.

Many researchers agree that standard soil corrosivity characterization techniques cannot be applied to aggregates, including Thapalia et al. (2011), who found when using the United States geotechnical surveying leachate tests that different particle sizes within the aggregate exhibit different electrochemical properties. The smaller particles have a larger surface area per unit volume and thus exhibit a higher conductivity at the surface over the coarse particles. Therefore, KDOT implemented the limitation of 5% passing the No. 200 sieve of the aggregate. Additionally, Brady et al. (2016) recommended the proposed test ASTM CXXX-XX and the advised tests by Edlerback and Beske (2014) be used when testing aggregates up to 7 cm.

2.4 GALVANIZED STEEL REINFORCEMENT CORROSION

As freshly galvanized steel is exposed to an aerated environment, oxidation of the zinc begins, forming a film of zinc oxide. Once the steel has been placed in the ground and left for a period of time zinc carbonate forms. This is the grey (graphite) colored film that is seen when one looks at aged galvanized steel placed in ground. The process of galvanizing an outer layer of zinc oxide and underlying alloy layers. Even if the zinc protection layers are breached, cathodic protection still prevents the corrosion of the steel as the steel is forced to be the cathodic couple in the presence of zinc. Galvanization using zinc is an environmentally friendly method of corrosion protection: since zinc is a naturally occurring element found in most soils, there is no contamination potential. Inspections of MSE structures located throughout the United States suggest that the AASHTO-developed linear weight loss model currently used to predict the amount

of sacrificial metal needed to serve the design life is conservative, since it is based on several methods used to test different metal loss models (Gladstone et al., 2006; Elias et al., 2009). As a result, highway agencies can potentially reduce the steel cost component of MSE walls by increasing the design life for galvanized steel and thus reducing the amount of steel required to achieve the design life.

CHAPTER 3: RESEARCH SCOPE

This chapter contains descriptions of the scope of work for this research, the materials used, and the tests conducted. The proposed ASTM aggregate resistivity test CXXX-XX and the new polycarbonate (Suffusion Box) are both used.

3.1 MATERIALS USED

Five backfill samples were collected from five KDOT-approved quarries as shown in Table 3.1.

Table 3.1: Sample Collection Locations

Material	Collection Locations
4" x 3/16" MSE Production Split	Louisburg, Kansas (APAC)
3” MSE Wall Backfill	DeSoto, Kansas (Martin Marietta)
2 1/2" x 3/4" Production Split	Olathe, Kansas (HAMM)
3” MSE Wall Backfill	Kansas City, Missouri (Martin Marietta)
River Sand MSE Wall Backfill	Wichita, Kansas (Cornejo)

Material was manually collected in accordance with ASTM D75 unless noted otherwise. Staff at the Olathe Hamm quarry used a front loader to mix the stock pile prior to sampling. The sample was placed in five-gallon buckets and sealed to trap fines and moisture and to prevent material contamination. Approximately 350 kg of material from each quarry were collected.

3.2 LAB TESTS

The tests listed in Table 3.2 were used to characterize the five different materials collected from quarries. Additional information is provided in the following sections on tests for which no standard procedure has been established, or for which the procedures for an existing test were modified for the purposes of this research.

Table 3.2: Material Characterization Tests

Standard	Description
ASTM C136	Sieve Analysis
New ASTM Proposed	Aggregate Electrical Resistivity
ASTM D2216	Water Content

3.2.1 The New ASTM Aggregate Electrical Resistivity Test

The new ASTM CXXX-XX, *New Test Method for Measurement of Aggregate Resistivity Using the Two-Electrode Soil Box Method* proposed by John J. Yzenas Jr., was used to test electrical resistivity of larger aggregates. It was evaluated by Brady et al. (2016) and found to be more representative of field conditions than the AASHTO T 288 test, and the methodology has been adopted by KDOT for resistivity testing. Subsequent paragraphs describe the alteration of this procedure for different applications.

For all tests, the resistance was measured using the AEMC® Model 4620 ground resistivity meter. This resistivity meter meets the requirements of AASHTO T 288. At the start of each resistance test, the meter was calibrated and checked to determine the accuracy of reading by measuring the resistance of known electrical resistors. The AEMC meter has a maximum display limit of 2000 ohm. The range of this meter is often too low to measure the resistance for soils tested in the smaller polycarbonate boxes when using the proposed ASTM procedure, as the resistance will be out of range (high). However, the limit of 2000 ohm provides a sufficiently high resistivity for the NEMA and Suffusion Box and was used without incident for measuring the resistance for pass/fail-type testing using the two-point current test method. For all the tests, the box factors used for the calculation are shown in the last column of Table 3.3.

To calculate the resistivity of the material, the same procedure from AASHTO T 288 was implemented using the box factor. The box factor is the surface area of the stainless steel plates divided by the distance between the plates. This gives units of cm^2/cm, which reduces to cm.

3.2.2.1 New ASTM Test Boxes

Samples were tested in two different polycarbonate boxes. The dimensions are shown in Table 3.3. Figure 3.1 shows the NEMA Box and Figure 3.2 shows the Suffusion Box. The Suffusion Box factor within Table 3.3 is for a single pair of stainless steel plates. The height shown in Table 3.3 is the entire section height. The length and height of the steel plates within the Suffusion Box are symmetrical (30.48 cm).

Table 3.3: Electrical Resistivity Box Details

Box Name	**Height (cm)**	**Length (cm)**	**Electrode Separation (cm)**	**Box Volume (cm^3)**	**Box Factor (cm)**
NEMA	14.5	34.9	24.0	12,145	21.1
Suffusion	182.9	30.5	30.5	169,901	30.5

Figure 3.1: NEMA Electrical Resistance Box

The NEMA Box is a repurposed commercial polycarbonate electrical box. Stainless steel electrode plates and the drain plug were installed by Zach Brady at KU. The drain hole, which consists of a threaded 9.5-mm-diameter plastic drain plug, was installed to allow water in the box to drain fully. The polycarbonate sheeting for the NEMA Box is thick and rigid enough to avoid deformation during the compaction process. The NEMA Box is sealed with silicone to prevent liquid inflow behind the steel plates.

Figure 3.2: Suffusion Electrical Resistance Box

The Suffusion Box was constructed using half-inch polycarbonate sheets. The internal dimensions of the box are 30.5 by 30.5 by 182.9 cm. The box has three pairs of 30.5-by-30.5-cm steel plates. The middles of the stainless steel plates are located 20, 86, and 155 cm from the bottom of the Suffusion Box. The metal sheets are connected to the polycarbonate with marine silicate. The drain bottom is 1.3 cm from the bottom of the box and is threaded into the polycarbonate bottom front panel. The drain is a plastic valve. The front of the Suffusion Box is a detachable polycarbonate panel to facilitate easy removal of material after testing. The front is sealed with a quarter-inch-thick rubber sheet between that polycarbonate panel and the main box. At the base of

the Suffusion Box, a perforated polycarbonate panel supported by half-inch polyvinyl chloride pipes was topped with a non-woven KDOT approved geotextile filter to minimize the loss of fines and coarse aggregate through the draining process; this panel is shown in Figure 3.3.

Figure 3.3: Bottom Section for Ease of Drainage within Suffusion Box

The geotextile is similar to what would be found around drainage pipes within MSE walls. The perforated panel was connected to the PVC with silicone. Figure 3.4 shows the typical setup during the running of suffusion tests and for resistance/resistivity measurements. In addition, the NEMA Box was run in conjunction with the Suffusion Box.

Figure 3.4: Test Setup during Suffusion Tests and Resistance Measurements

3.2.2.2 New ASTM Aggregate Resistivity Test Procedure

Material taken from the quarry stockpile was first inspected so a homogenous sample could be tested within the NEMA Box. In addition, the test material was inspected for foreign objects such as leaves, grass, or plastics. The selection of material for the NEMA Box matched what was placed within the Suffusion Box. The material was placed into the NEMA Box in 5- to 7-centimeter layers. Each layer was compacted by alternately lifting and dropping each side of the box, approximately 25 drops per layer. The final layer was level with the top of the NEMA Box. In some cases, achieving a level surface required striking off excess with a straight edge. The box was then filled with deionized (DI) water. When DI water was at the top of the NEMA Box, it was assumed the saturation was at 100%. During soaking, minor amounts of DI water were added when necessary to keep the water level even with the top of the steel plate within the NEMA Box to maintain 100% saturation. The additional water was needed to replace water lost to evaporation.

Immediately after the box was filled with DI water, resistance measurements were taken for 24 hr at a series of time intervals. For the first 1 to 2 hr, measurements were taken at 5- to 10-min intervals to capture the initial trend of resistance, and, as time progressed and the resistance stabilized, measurements were taken at less frequent intervals. After a soaking period of 24 hr, the NEMA Box was allowed to fully drain. Full drainage was assumed to have occurred when no more pore fluid was observed to drop out of the drain hole. In order to achieve complete drainage, the opposite end of the box from the drain hole was elevated by 1 inch. Immediately after full drainage, the resistance was measured for 24 hr at various increments of time. The same technique used for measurements for the saturated cycle was implemented here. The NEMA Box was left uncovered during the drained cycles.

For the first two test materials only, the saturated cycle was recorded initially. NEMA Box resistivity tests of Materials 3 to 5 included the 24-hr +/- resistance measurements for saturated and drained cycles. Reconstituted samples of Materials 1 and 2 were tested within the NEMA Box to get both the saturated and drained cycles. For this second round of NEMA testing, Material 1 was composed of aggregate from the top, middle, and bottom from the Suffusion Box after the aggregate had undergone the saturated and drained tests. The material collected from the Suffusion Box was mixed in a large 20-gallon container that was rolled on the ground. Then, the material was transferred from the 20-gallon container to 5-gallon buckets, where it was shaken and then mixed again in the 20-gallon container to create an evenly distributed gradation sample for testing within the NEMA Box. For Material 2, extra original material was used for the second round of NEMA testing.

Samples were soaked, permitted to drain, and soaked again in a series of three to five cycles to simulate repeated infiltration cycles in the field. The material soaked and drained in the first cycle (Cycle 1) was the same material initially used for the first soaked test. Cycle 2 material was the material from Cycle 1 after saturation and drainage. No material was removed or added to the system. The saturated and drained cycles continued until the end of the test for each material listed in Table 3.1.

3.2.2.2.1 New Suffusion Box Test Procedure

The material tested within the Suffusion Box was a representative sample taken from a quarry stockpile, and the same quarry sample was used to provide material for the Suffusion Box and the NEMA Box. The test material was inspected for foreign objects such as organics and plastics. The test material was placed within the sealed Suffusion Box by using a tremie pipe. The pipe shown in Figure 3.4 was used in all tests except for Test 1, when the material was

poured directly into the box. The tremie pipe was used to help obtain repeatable and consistent placement of the materials listed in Table 3.1.

Figure 3.4: Tremie Pipe Used in Suffusion Box

The amount of aggregate added for each layer tremied was roughly 15 L. The tremie pipe was moved up during filling until it was close to the top of the Suffusion Box. For the uppermost portion of the box, hand-poured material was added to bring the fill flush with the top of the box.

The box was then filled with DI water level to the top of the box. During the filling process, once the water was immediately level with the top of each steel plate, the resistance would be measured. The aggregate was assumed to be at 100% saturation once the water level was at the

top of the box. The resistance was measured during the saturation cycle for 24 hr +/- 1 hr. For the first 1 to 2 hr, measurements were taken at 5- to 10-min intervals to capture of initial trend of the change in electrical resistance. As time progressed, the trend flattened and therefore measurements were taken at longer time intervals. After the saturation cycle, the valve was opened and water was allowed to fully drain from the box via gravity. The resistance was measured immediately after the water level dropped beneath the steel plates. The resistance was measured at the three locations for 24 hr +/- 1 hr. The same technique used for measurements within the NEMA Box for the saturation cycle was followed for the Suffusion Box. Once the saturated and drained resistance had been measured for 24 hr, Cycle 1 was considered complete. The saturated and drained cycles were repeated an additional two to four times for a total of three to five cycles.

CHAPTER 4: TEST RESULTS

This chapter contains a discussion of the results of grain size distribution, moisture content, and resistivity testing of the sampled materials. The acceptable aggregate gradation range is taken from the specifications in KDOT Section 1107, "Aggregates for Backfill," and is shown in Table 4.1. An example of the limits is graphed on Figure 4.1.1a and in all other initial grain size distributions. The acceptable region is the area between the lower and upper bounds (orange and blue lines).

Table 4.1: Grain Size Distribution Requirements for MSE Wall Backfill

Aggregates for Panel MSE Wall Backfill Percent Passing Square Mesh Sieves		
4 in.	No. 40	No. 200
100	60–100	0 –5

Section 4.1 contains a comparison of quarry-provided grain size distributions and the sample grain size distributions as tested in lab. In addition, the grain size distributions from the Suffusion Box for the top, middle, and bottom sections were determined after the completion of the suffusion tests to estimate the amount of migration between the layers. The Suffusion Box material was sieved and tested after completion of the saturated and drained cycles. Resistivity values determined following the proposed ASTM test protocol using the NEMA resistivity box are then presented, along with the resistivity results from the Suffusion Box. The NEMA resistivity was used as a reference to validate the resistivity results from the Suffusion Box. The minimum resistivity standard from KDOT Section 1107, "Aggregates for Backfill," for MSE wall backfill is 3000/5000 ohm-cm, and this limit is noted on all resistivity plots.

4.1 Grain Size Distribution and Moisture Content

4.1.1 Test 1 Material Material 1 was collected from Louisburg, Kansas. Figure 4.1.1a shows the quarry-provided grain size data along with the results from two lab sieve analyses. The results from Figure 4.1.1a show the in-lab sieve had more fines than the quarry data. The percentages passing the No. 40 and 200 sieves from the quarry test are not given; however, the lab sample results were 8 and 5%, respectively.

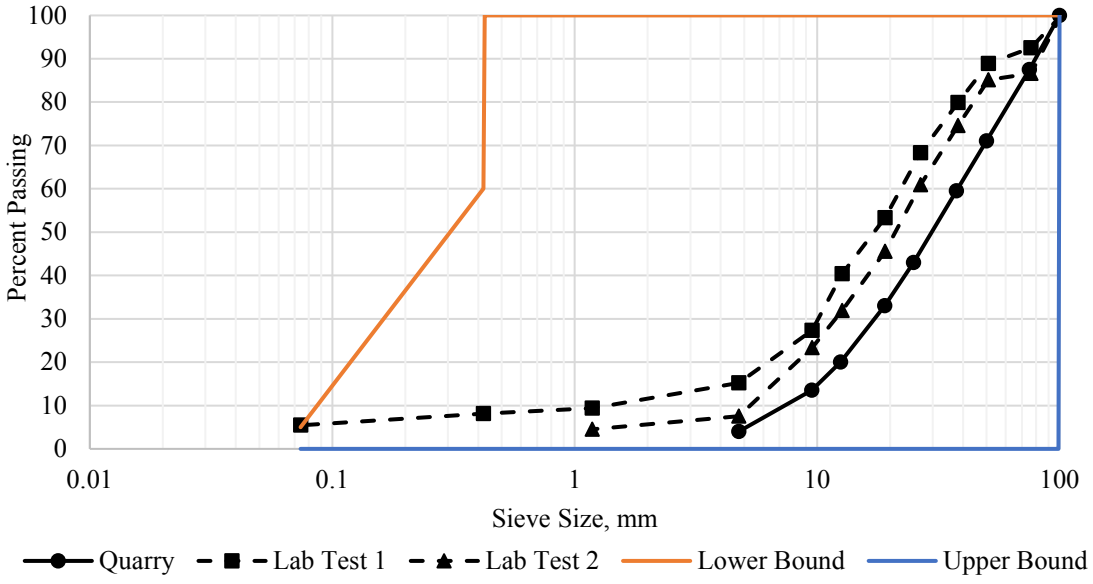

Figure 4.1.1a: Grain Size Distribution for Material 1

Figure 4.1.1b contains the grain size distribution results from the Suffusion Box after cyclic testing for three different depths (top, middle, and bottom). The percentages passing the No. 40 sieve from top to bottom were 2.0, 3.5, and 5.9%, respectively. The percentages passing the No. 200 sieve from top to bottom were 1.3, 1.9, and 2.9%, respectively. Some fines were apparently washed out of the system during cycling, as the percentage passing the No. 200 sieve for the initial

bulk sample was 5%, while the measured fines contents for the material after cyclic testing were 1.3, 1.9, and 2.9% for the top, middle, and bottom of the box, respectively.

The moisture content of the material at the top of the box after testing and during sampling was 5.4%, and for the material at the bottom of the box the moisture content was 7.7%.

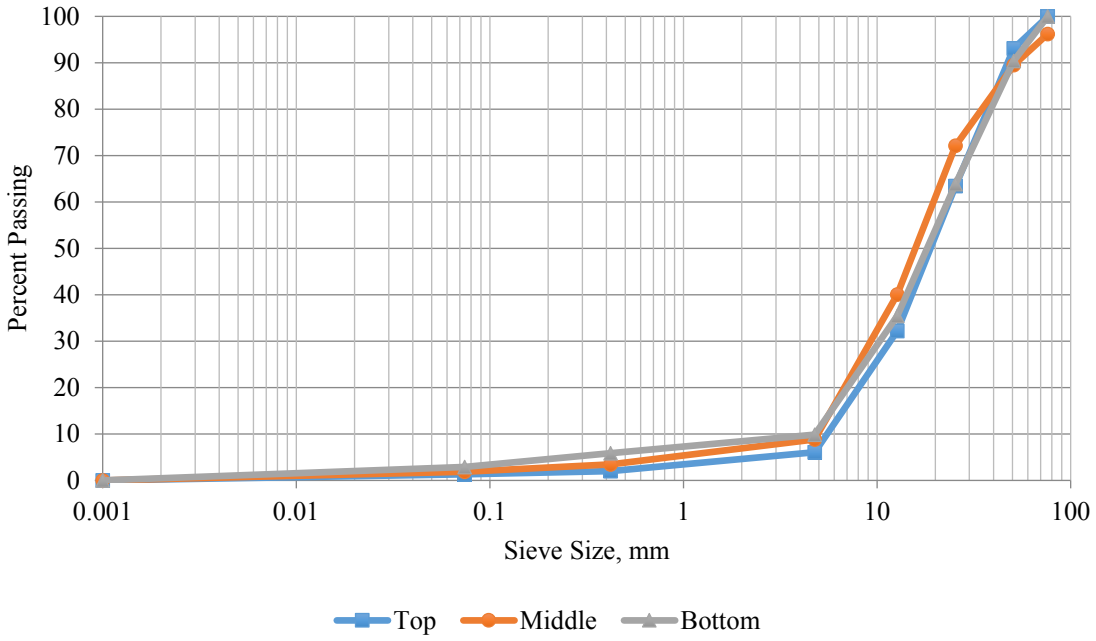

Figure 4.1.1b: Suffusion Grain Size Distribution at Different Locations for Material 1

4.1.2 Test 2 Material

Material 2 was collected from DeSoto, Kansas. Figure 4.1.2a shows the quarry-provided grain size data along with the results from the lab sieve analyses. The data shows the quarry-sieved material was somewhat finer than the material sieved in lab. The results from Figure 4.1.2a show the percentages passing the No. 4, 40, and 200 sieves during the quarry test were 20, 7, and 4.7%, compared to 9, 3, and 1% during the KU lab tests.

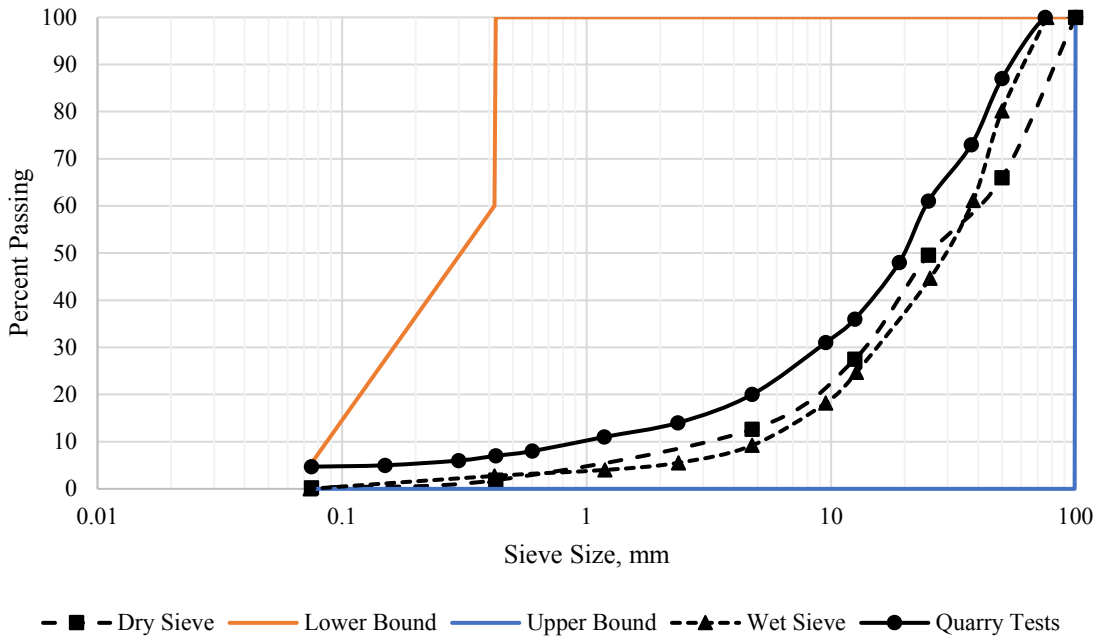

Figure 4.1.2a: Grain Size Distribution for Material 2

Figure 4.1.2b contains the grain size distribution results from the Suffusion Box after cyclic testing for three different depths (top, middle, and bottom). The percentages passing the No. 40 sieve from top to bottom were 2.2, 3.5, and 5.1%, respectively. The percentages passing the No. 200 sieve from top to bottom were 0.9, 1.2, and 1.9%. The percent passing the No. 200 sieve, used for reference, was 1% compared to the Suffusion Box sieve results from top to bottom of 0.9 to 1.9%. These results show that fines migrated through the voids of the material during the cyclic testing.

The moisture contents from within the Suffusion Box from top to bottom after testing were 4.8, 5.9, and 6.8%.

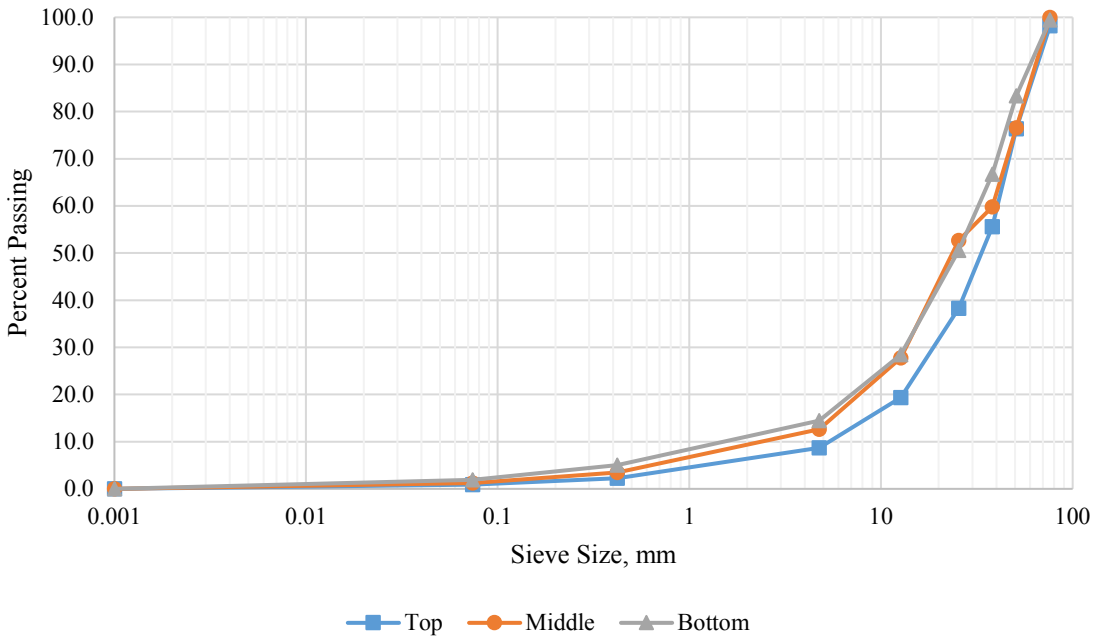

Figure 4.1.2b: Suffusion Grain Size Distribution at Different Locations for Material 2

4.1.3 Test 3 Material

Material 3 was collected from Olathe, Kansas. Figure 4.1.3a shows the quarry-provided grain size data along with the results from two lab sieve analyses. As shown in Figure 4.1.3a, the in-lab sieves show a higher percentage of fines compared to the bulk data provided by the quarry. The percentages passing the No. 4, 40, and 200 sieves during the quarry test were 1, 1, and 1%, compared to 3, 2, and 0.1% during in-lab sieve analysis.

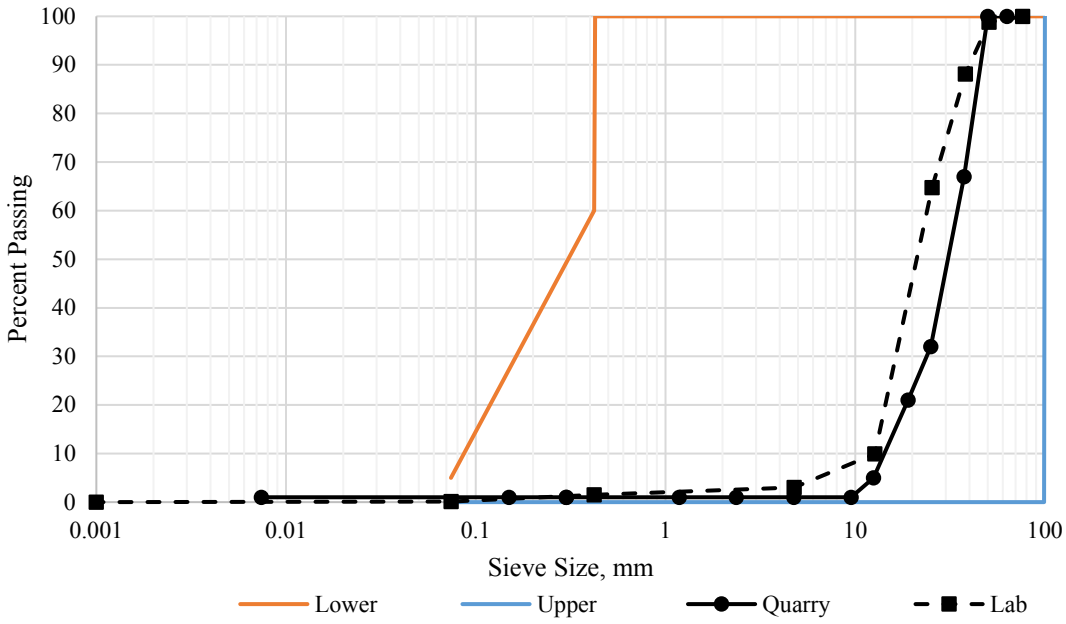

Figure 4.1.3a: Grain Size Distribution for Material 3

Figure 4.1.3b contains the grain size distribution results from the Suffusion Box after cyclic testing for three different depths (top, middle, and bottom). The percentages passing the No. 40 sieve from top to bottom were 0.5, 0.8, and 2.7%, respectively. The percentage passing the No. 200 sieve from top to bottom was 0.3, 0.5, and 1.6%, respectively. Judging from these results, suffusion occurred, leading to a higher percentage of fines at the base of the Suffusion Box.

The moisture contents from top to bottom were 3.7, 4.3, and 5.2%.

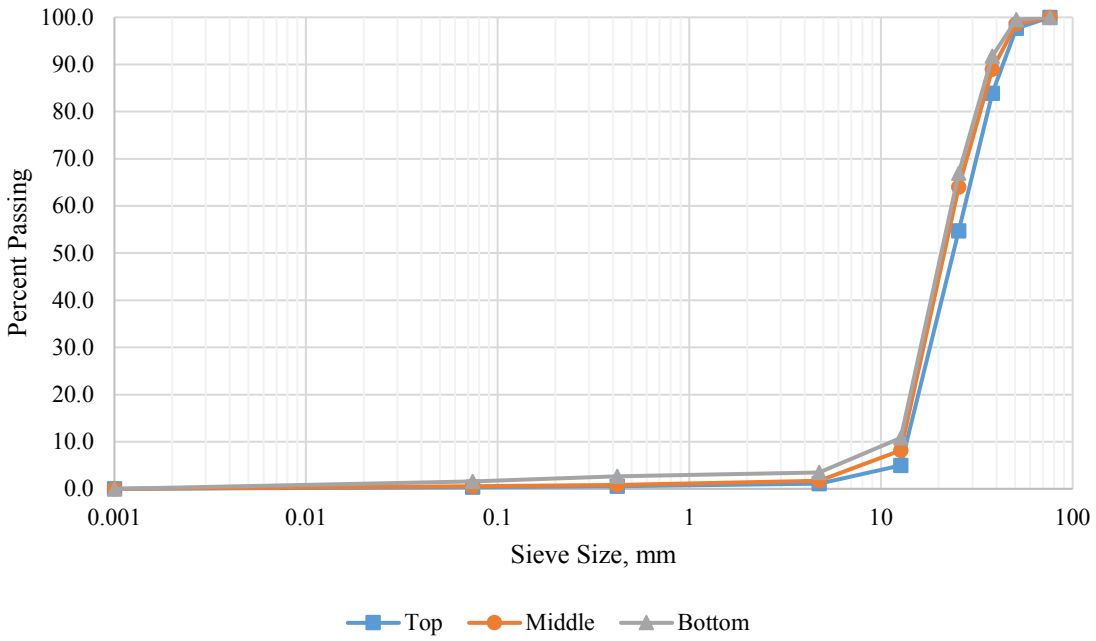

Figure 4.1.3b: Suffusion Grain Size Distribution at Different Locations for Material 3

4.1.4 Test 4 Material

Material 4 was collected from Kansas City, Missouri. Figure 4.1.4a shows the quarry-provided grain size data along with the results from two lab sieve analyses. As shown in Figure 4.1.4a, the bulk percentages of smaller aggregate and fines were somewhat larger for the lab sieve than reported by the quarry. The percentages passing the No. 40 and 200 sieves from the quarry data were 10 and 0.5%, compared to 7 and 3% for the in-lab tests.

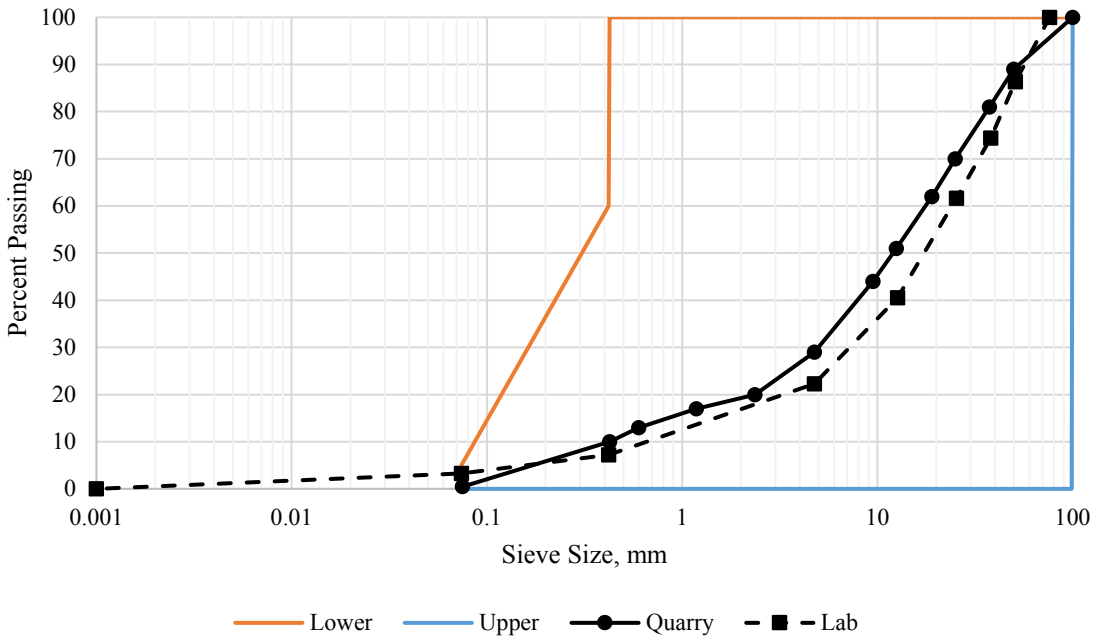

Figure 4.1.4a: Grain Size Distribution for Material 4

Figure 4.1.4b contains the grain size distribution results from the Suffusion Box after cyclic testing for three different depths (top, middle, and bottom). The percentages passing the No. 40 sieve from top to bottom were 6.4, 6.3, and 9.6%, respectively. The percentages passing the No. 200 sieve from top to bottom were 3, 3.1, and 5.3%, respectively. Judging from these results suffusion took place, leading to a higher percentage of fines toward the bottom.

The moisture contents from top to bottom were 4.9, 4.9, and 5.9%.

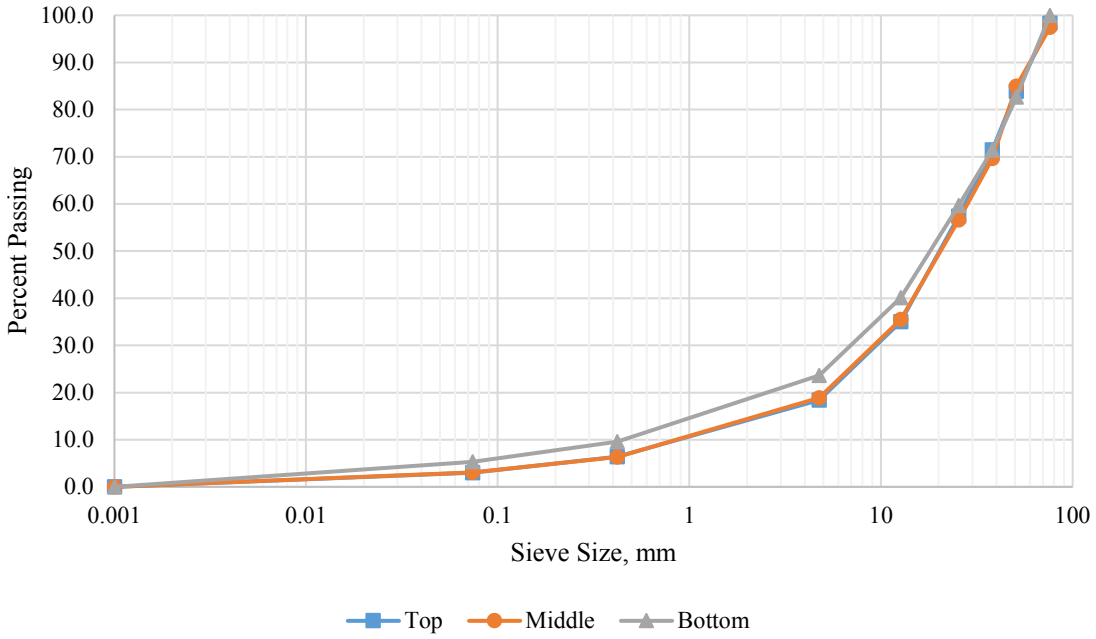

Figure 4.1.4b: Suffusion Grain Size Distribution at Different Locations for Material 4

4.1.5 Test 5 Material

Material 5 was collected from Wichita, Kansas. Figure 4.1.5a shows the quarry-provided grain size data along with the results from two lab sieve analyses. The results from Figure 4.1.5a show the in-lab sieve analyses find somewhat more fines than the quarry data. The percentages passing the No. 40 and 200 sieves were 32 and 0% for the quarry data, respectively. The percentages passing the No. 30, 50, and 200 sieves were 43, 15, and 4% for the in-lab data, respectively. The percentage passing the No. 40 from the lab data is 29%, as estimated in Figure 4.1.5a.

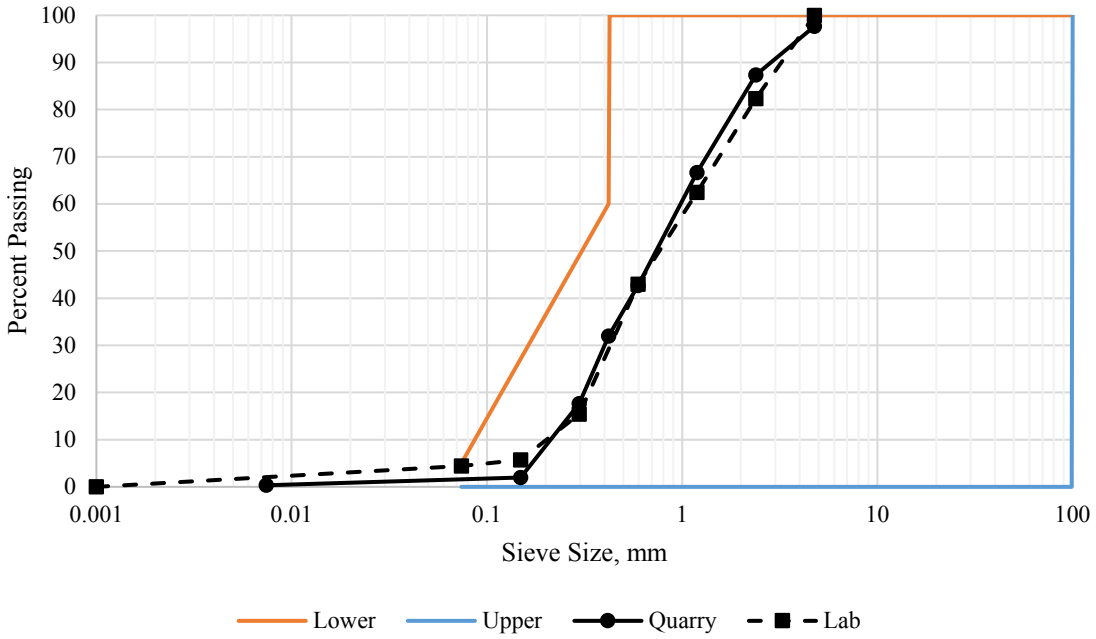

Figure 4.1.5a: Grain Size Distribution for Material 5

Figure 4.1.5b contains the grain size distribution results from the Suffusion Box after cyclic testing for three different depths (top, middle, and bottom). The estimated percentages passing the No. 40 sieve from top to bottom were 28, 28, and 29%, respectively. The percentages passing the No. 200 sieve from top to bottom were 0.42, 0.33, and 0.37%, respectively. The results show that after the cycles had been completed for testing, very little finer material suffused downward. The small amount of change in percentage fines from top to bottom could be a result of the slower water velocity in the sand having less dislodging energy and the smaller void space between grains, which caused the vertical permeability to decrease.

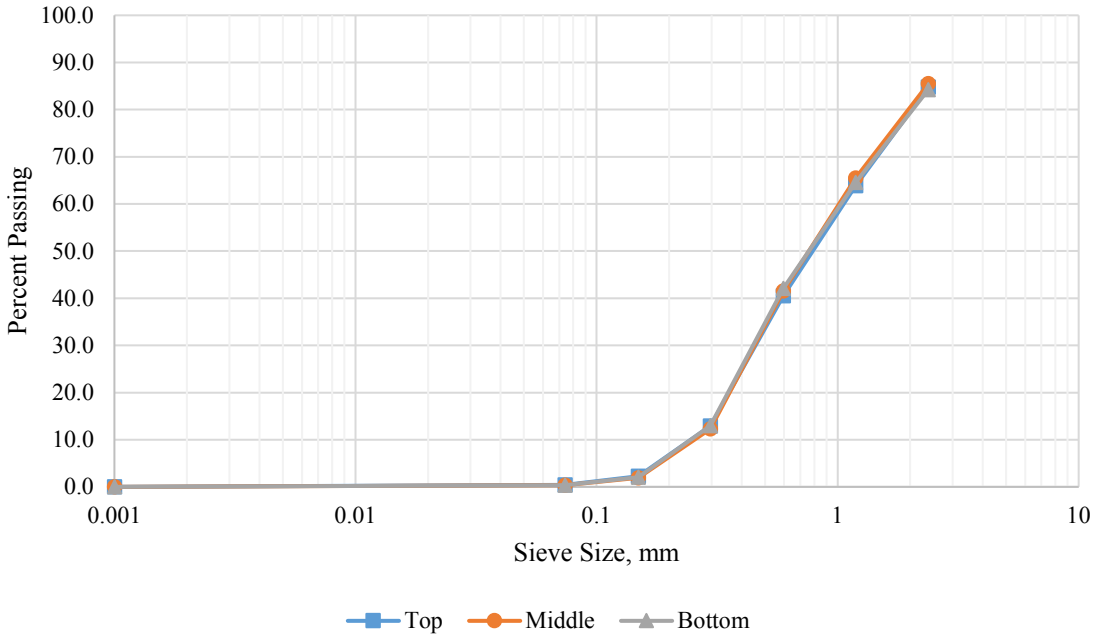

Figure 4.1.5b: Suffusion Grain Size Distribution at Different Locations for Material 5

4.2 ASTM (NEMA Box) Resistivity

The ASTM CXXX-XX procedure was used to determine aggregate resistivity. This test is believed to be more representative of field conditions than AASHTO T 288, and AASHTO T 288 may yield unrepresentative results for larger aggregate sizes (Brady et al., 2016). The test was performed on five samples from KDOT-approved quarries. The first two tests included six to seven saturated cycles, and the other tests had three to four saturated cycles. For some drained cycles the resistivity measurement was so high it exceeded the resistance meter limit (2000 ohms), thus leading to a smaller amount of graphed cycles. These measurements are reported as exceeding the limit, where applicable.

Each resistivity (NEMA Box) test was conducted with approximately 23 to 25 kg of dry material. The resistivity measurements reported for each aggregate are from the 24-hour measurement.

4.2.1 Test 1 Material

Figure 4.2.1a shows the saturated resistivity measurements for the Louisburg, Kansas material. Saturated testing was conducted on two samples; results for both are shown in Figure 4.2.1a. Saturated resistivity was generally stable within a given round but increased substantially with each cycle for both samples. The results show that, the lowest resistivity, 2382 ohm-cm, occurred at 24 hr during saturation Cycle 1, and the highest was 4093, from Cycle 3 at 24 hr, an increase of 72%. It is notable that Cycle 3 for Sample 1 (Sat 3 R1) had a higher resistivity measurement than Cycle 4. This suggests that the flushing effect from the cycling of water was no longer having a significant effect on the resistivity after Cycle 3.

For the drained condition within the NEMA Box, the initial resistance measurement was above 2000 ohms (the maximum for the AEMC device); therefore, the resistivity was above 42,200 ohm-cm.

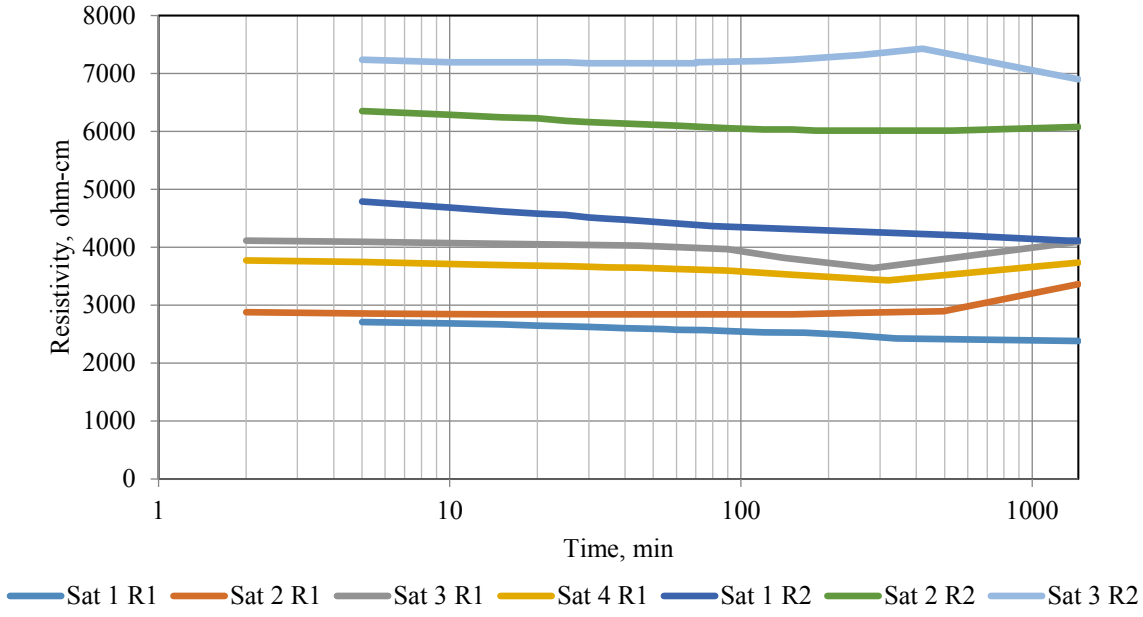

Figure 4.2.1a: Saturated NEMA Box Resistivity Measurements on Material 1

4.2.2 Test 2 Material

Figure 4.2.2 shows the saturated resistivity within the NEMA box for the aggregate from DeSoto, Kansas. For this material only, data for the saturated cycle was recorded for the first round of data; therefore, the testing was repeated, and, as shown in Figure 4.2.2, there are two rounds of data points for the saturated testing. As with Material 1, the figure shows that resistivity was largely stable within a given round (with some minor declines over time), but there was a substantial increase in resistivity as the number of cycles increased. The saturated resistivity values for Sample 1 taken after 24 hr of saturation for cycles 1 to 3 (Sat 1 R1, Sat 2 R1, Sat 3 R1) were 2045, 2473, and 3376 ohm-cm, respectively. The saturated measurements for Sample 2 taken at 24 hr for cycles 1 to 3 were 5233, 5950, and 6203 ohm-cm, respectively. This shows an increase in resistivity as the number of cycles increased.

For the drained condition within the NEMA box, the initial resistance measurement was above 2000 ohms; therefore, the resistivity was above 42,200 ohm-cm.

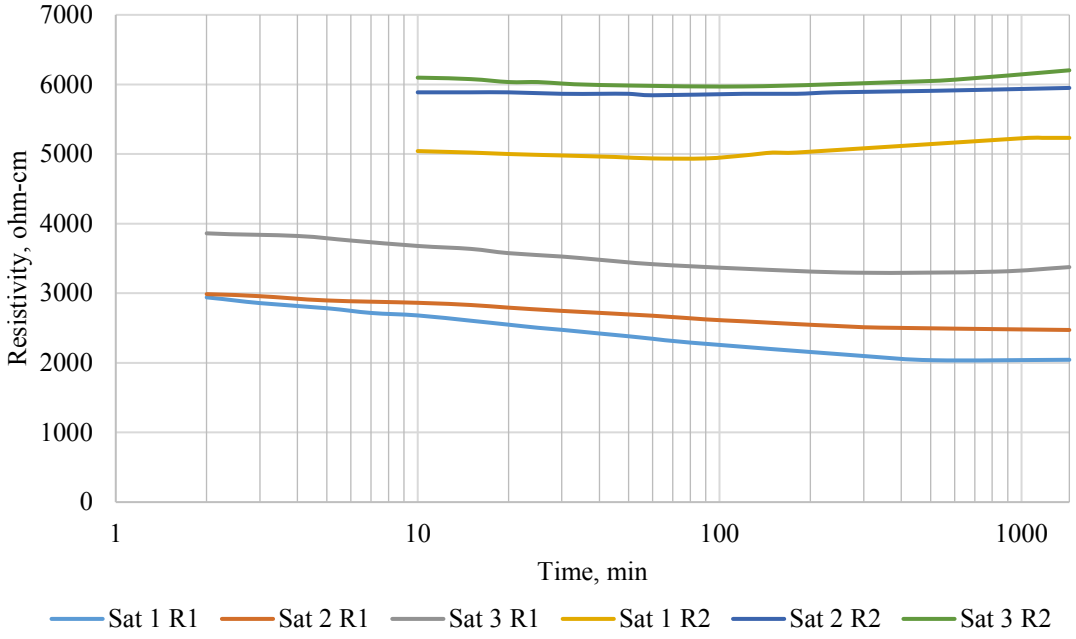

Figure 4.2.2: Saturated NEMA Box Resistivity Measurements on Material 2

4.2.3 Test 3 Material

The material tested was from Olathe, Kansas. Figure 4.2.3a shows the resistivity trends after saturation for three saturated cycles. Resistivity decreased during each saturated cycle but increased substantially from cycle to cycle. The lowest resistivity measured after 24 hr was 1359 ohm-cm for Cycle 1, and the highest was 2977 for Cycle 3.

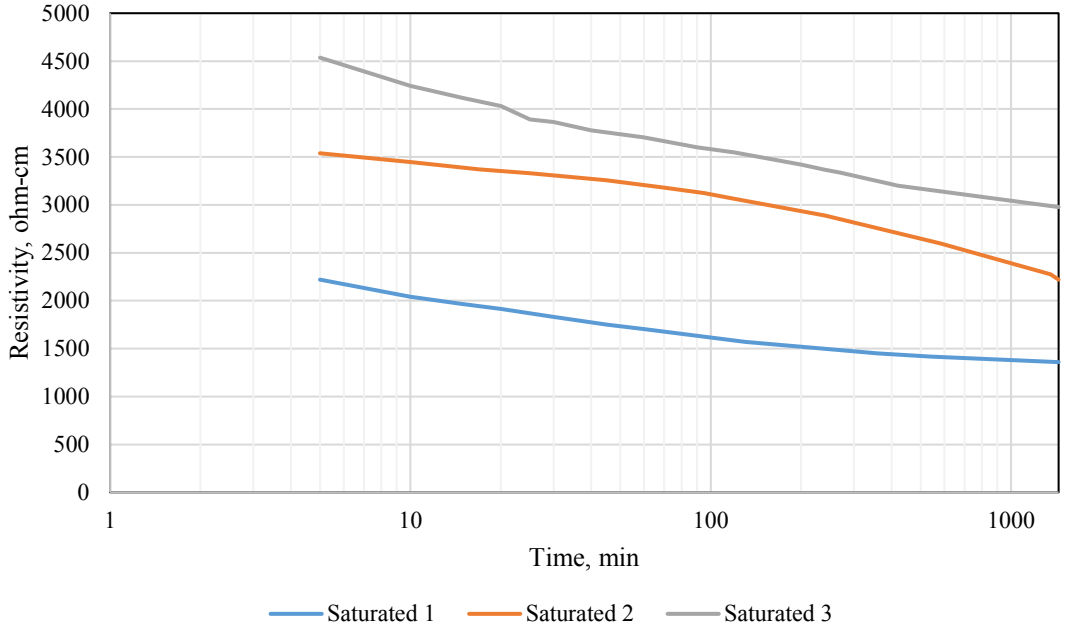

Figure 4.2.3a: Saturated NEMA Box Resistivity Measurements on Material 3

Figure 4.2.3b shows the drained resistivity for Material 3. As the number of cycles increased, the resistivity increased. The only cycle for which a drained measurement of resistance could be taken after 24 hr was Cycle 1, which was 21,775 ohm-cm. Cycles 2 and 3 reached the maximum resistance measurement at approximately 120 and 5 min, respectively.

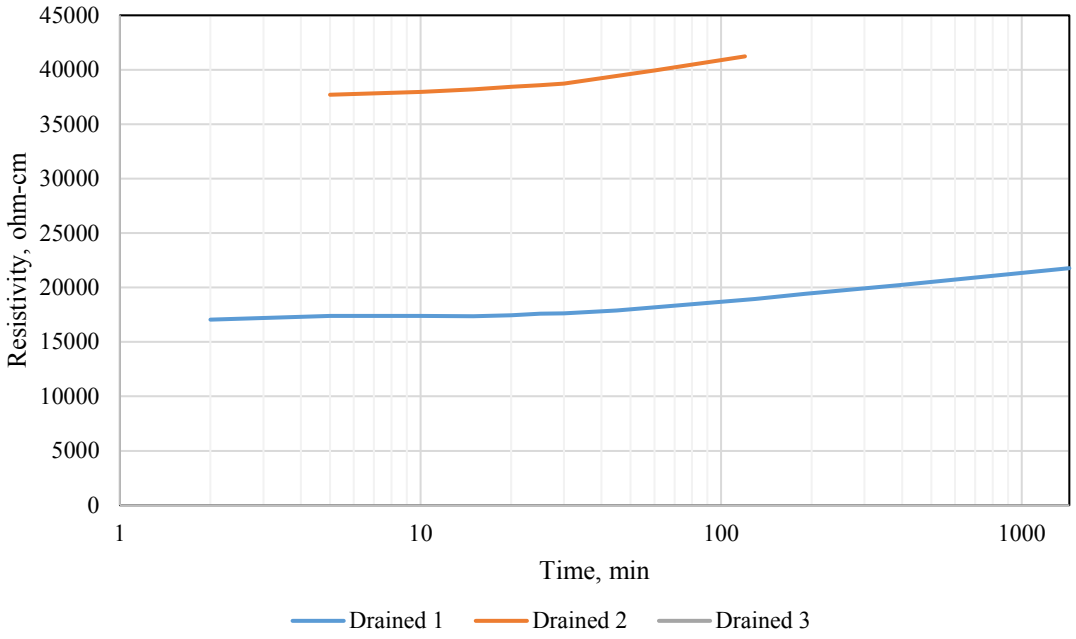

Figure 4.2.3b: Drained NEMA Box Resistivity Measurements on Material 3

4.2.4 Test 4 Material

The material tested was Kansas City, Missouri aggregate. Figure 4.2.4a is for the saturated cycles, and shows that resistivity declined somewhat throughout individual cycles, with the exception of the 24-hr measurement for Cycles 2 and 4, which increased from the previous measurements within that cycle. Figure 4.2.4a also shows a substantial increase in resistivity as the number of cycles increased. The lowest resistivity measurement at 24 hr was 2711 ohm-cm for Cycle 1, and the highest was 8398 ohm-cm for Cycle 4. Figure 4.2.4b is for the drained cycles; it also shows a substantial increase in resistivity as the number of cycles increase. The lowest measured resistivity at 24 hr was 12,766 ohm-cm for Cycle 1, and the highest was 30,890 ohm-cm for Cycle 4, a 142% increase over Cycle 1.

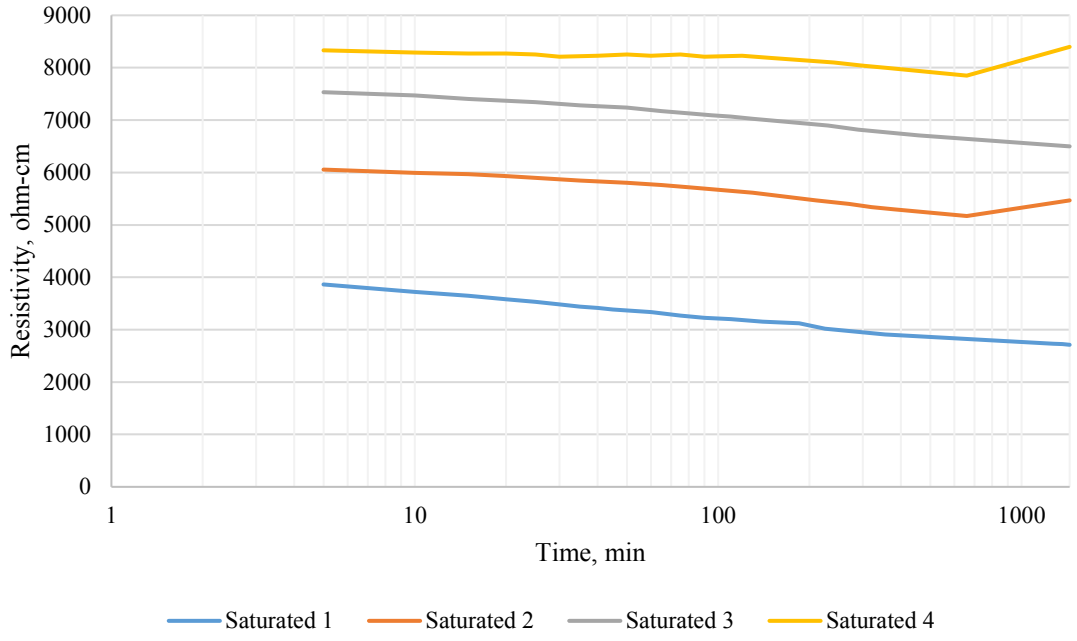

Figure 4.2.4a: Saturated NEMA Box Resistivity Measurements on Material 4

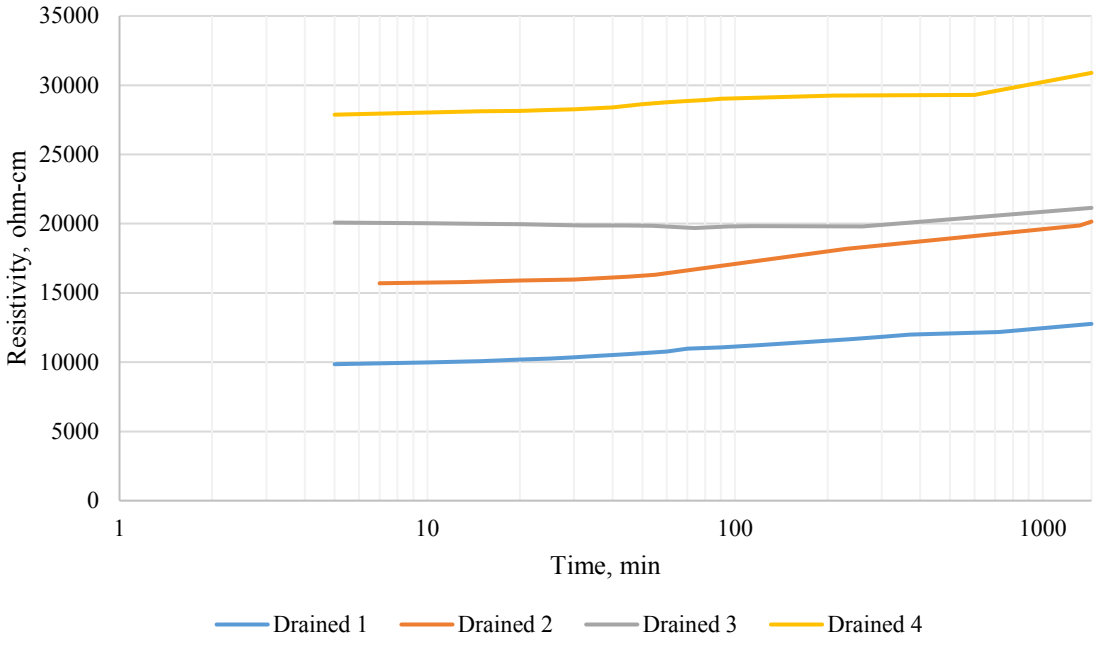

Figure 4.2.4b: Drained NEMA Box Resistivity Measurements on Material 4

4.2.5 Test 5 Material

Figure 4.2.5a shows the saturated resistivity measurements for the Wichita, Kansas material. Resistivity was very stable for a given cycle; however, unlike for the other materials, saturated resistivity declined between Cycles 1 and 3. Cycle 4 was relatively unchanged from Cycle 3. Judging from the results, the lowest resistivity at 24 hr occurred for the saturated Cycle 3 at 11,668 ohm-cm. All measurements recorded for the saturated condition are above the 3000/5000-ohm-cm limit established by KDOT.

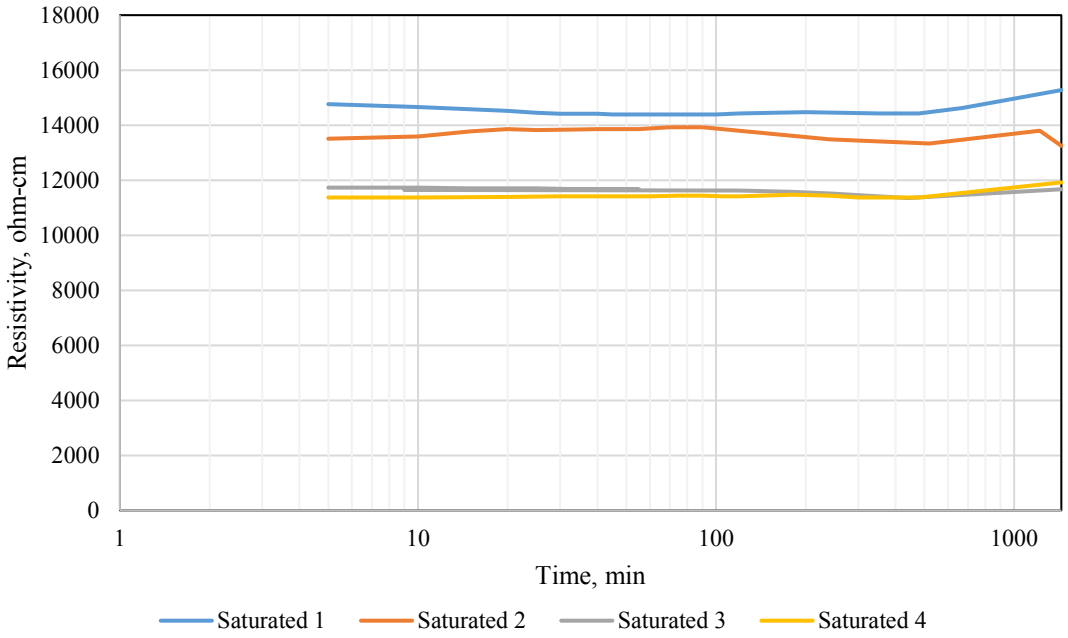

Figure 4.2.5a: Saturated NEMA Box Resistivity Measurements on Material 5

Figure 4.2.5b shows the drained resistivity measurements. Unlike for the other materials, the drained resistivity values decreased with time for the first three cycles before stabilizing for Cycle 4. The results show that the lowest resistivity measurement at 24 hr was for Cycle 3 at 12,783 ohm-cm, which exceeds the KDOT minimum of 3000/5000 ohm-cm. The range of values at 24 hr for the drained cycles was approximately 13,000 to 17,500 ohm-cm.

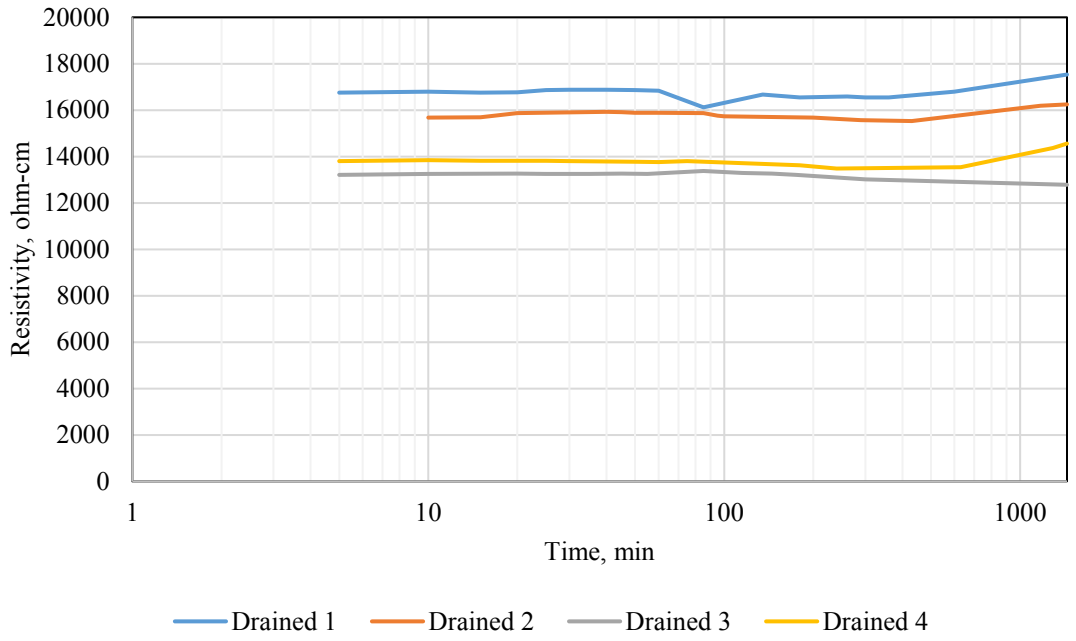

Figure 4.2.5b: Drained NEMA Box Resistivity Measurements on Material 5

4.3 Suffusion Box Resistivity

The Suffusion Box is a polycarbonate box designed at KU to provide multiple resistivity measurements in a column of aggregate to better simulate field conditions and determine the significance of suffusion on resistivity. Measurements are taken at three locations within a column of aggregate. The distances to the centers of the 30.5-by-30.5-cm stainless steel plates at these locations as measured from the bottom of the box are 20, 86, and 155 cm. Each aggregate went through a series of saturated and drained cycles, with the saturated and drained steps lasting 24 hr each. The following sections contain the resistivity measurements taken at three different elevations within the box. Due to the unique configuration of the plates within the box, resistivity values for the materials are likely greater than those measured using this method; therefore, the values shown are likely conservative. However, positions of the resistivity trends relative to each

other should not have been affected, and they can be used for comparisons. Corrections factors have been developed and are discussed in detail in Chapter 5.

4.3.1 Test 1 Material

Test 1 material was from Louisburg, Kansas. Figure 4.3.1a shows the measured results for the saturated cycles for the material. Measured resistivity was generally stable for a given set of electrodes during a given cycle, with a slight general downward trend during the 24-hr period. Within a given cycle, resistivity values at the different elevations were fairly close. Resistivity increased substantially between cycles. As shown in Figure 4.3.1a, the results from Cycles 1 and 5 are: 1518 to 2438 ohm-cm for the top layer, 1500 to 2451 ohm-cm for the middle layer, and 1740 to 2819 ohm-cm for the bottom layer.

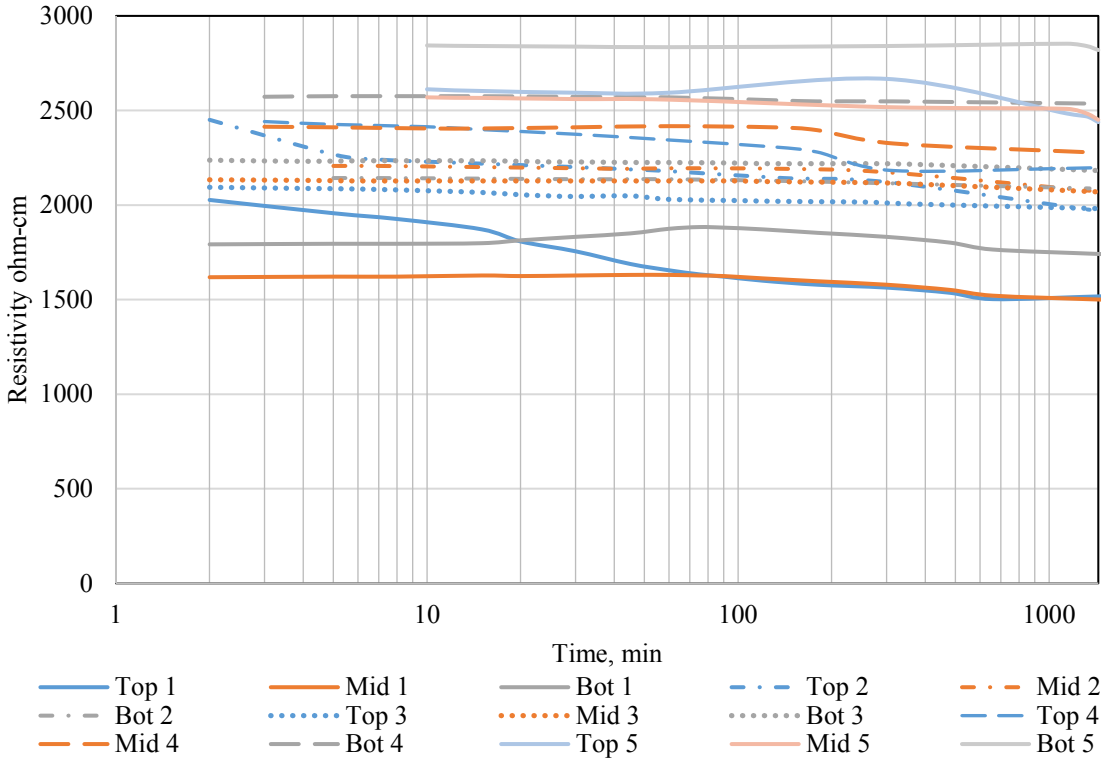

Figure 4.3.1a: Saturated Suffusion Box Resistivity Measurements on Material 1

Figure 4.3.1b contains the measured resistivity values for the 24-hr drained cycles within the Suffusion Box (for the first cycle, the duration of measurements stops at 1300 min). The results show that the lowest resistivity values were recorded during Cycle 1 for all three locations. The measured resistivity was above the recommended value of 5000 ohm-cm for all measurements during all cycles. However, measurements differed greatly based on position in the column as the number of cycles increased. Resistivity values increased dramatically for the upper and, to a lesser degree, for the middle portion of the fill, while resistivity values near the base of the fill increased to a much smaller degree. Additionally, resistivity values increased substantially during each cycle for the upper and middle portions of the sample, while they decreased slightly for the lower portion of the sample. This is likely due to ongoing residual drainage activity which was reducing the water content in the upper and middle portions of the box, while the increased fines content in the lower portion was facilitating greater water retention in the bottom portion of the box, keeping resistivity values low.

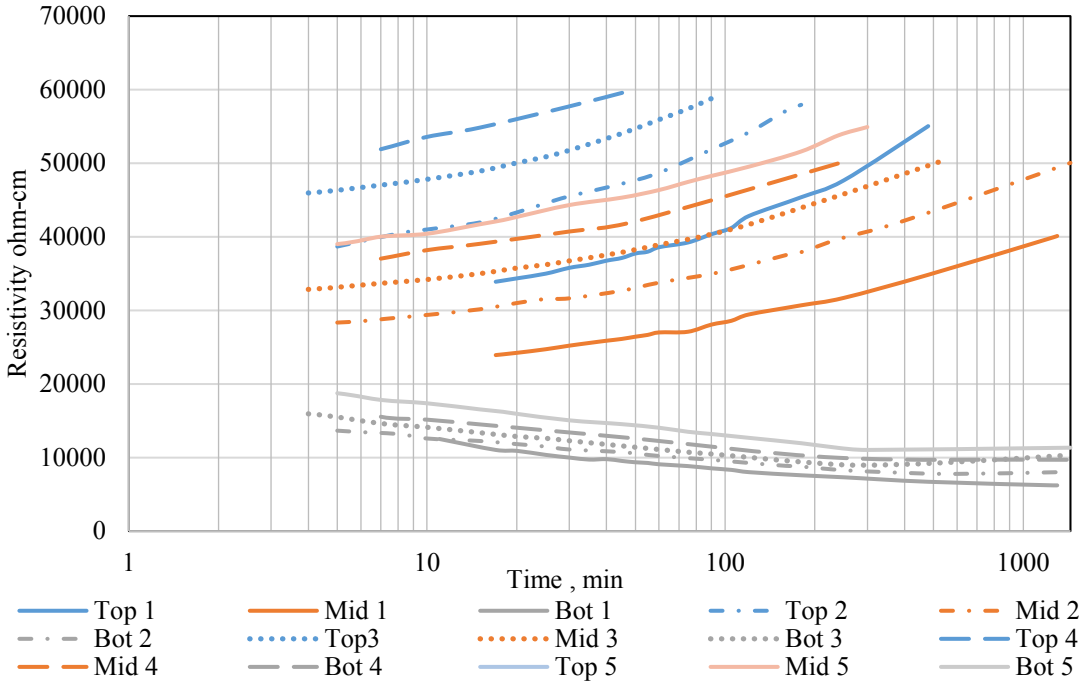

Figure 4.3.1b: Drained Suffusion Box Resistivity Measurements on Material 1

4.3.2 Test 2 Material

The material for Test 2 was collected from DeSoto, Kansas. Figure 4.3.2a shows the measured results for the saturated cycles. Resistivity values consistently decreased logarithmically with time throughout the 24-hr period. Resistivity increased substantially with each cycle. As shown in Figure 4.3.2a, the minimum resistivity values measured at 24 hr for each layer for cycles 1 through 4 were: 1430, 2280, 2941, 3414 ohm-cm for the top layer; 1100, 2268, 3170, and 3719 ohm-cm for the middle layer; and 1012, 1618, 2195, and 2713 ohm-cm for the bottom layer. For Cycle 2 the middle layer became more resistant that the top layer, so the middle layer for cycles 3 and 4 has higher resistivity than the top layer.

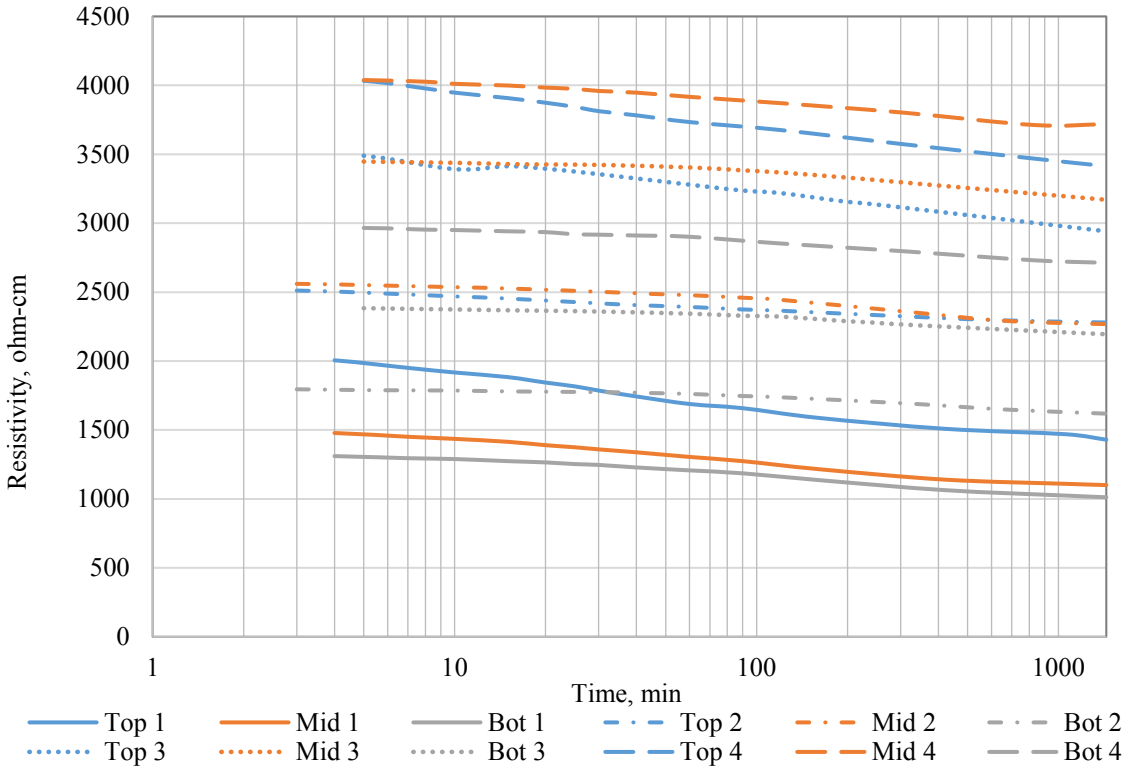

Figure 4.3.2a: Saturated Suffusion Box Resistivity Measurements on Material 2

As with Material 1, resistivity values were varied greatly according to elevation during the drained cycles. As shown in Figure 4.3.2b, the top layer reached the maximum resistance measurement from the AEMC device by the first cycle at 180 min. The middle layer reached the maximum reading in Cycle 2 at 780 min, and the bottom layer had measurements for all bottom layers. The resistivity measurements for the bottom layer from Cycles 1 to 5 after 24 hr were 4054, 6370, 6462, and 8077 ohm-cm. For a given cycle, resistivity values increased during the cycle for the upper portions of the sample and were stable or decreased slightly for the bottom portion of the sample.

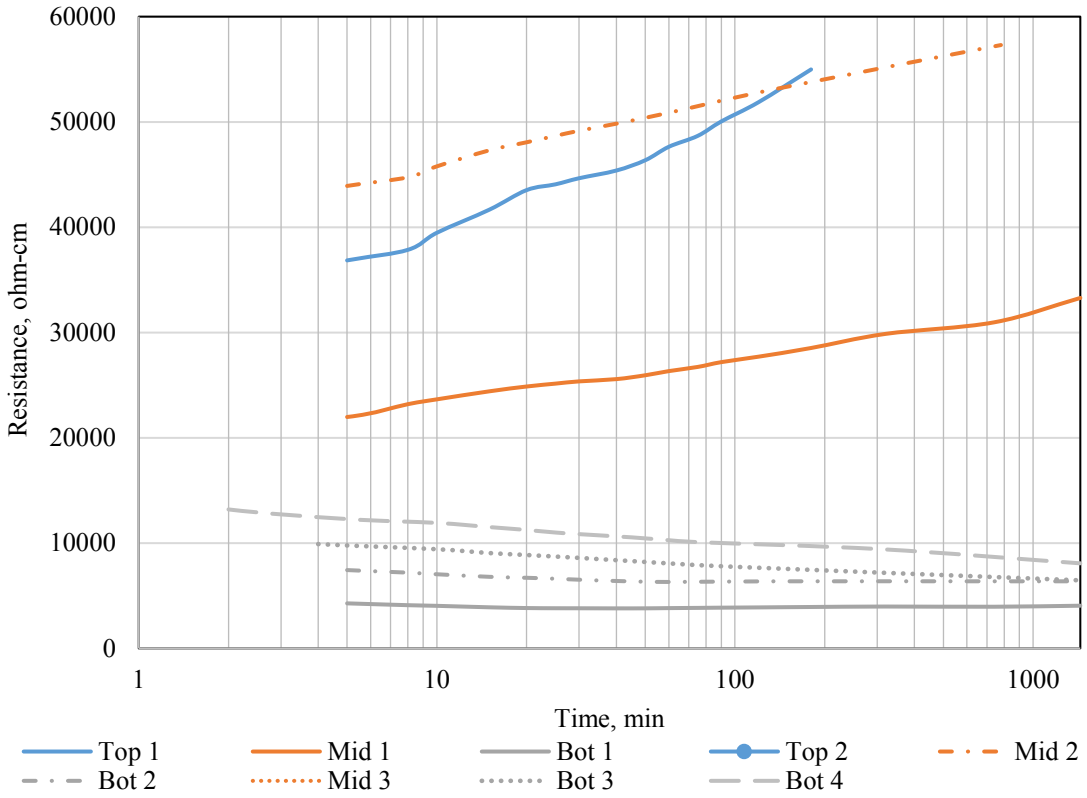

Figure 4.3.2b: Drained Suffusion Box Resistivity Measurements on Material 2

4.3.3 Test 3 Material

The material for Test 3 was collected from Olathe, Kansas. Figure 4.3.3a shows the saturated resistivity measurements. Resistivity values declined with time during each cycle; however, resistivity values increased substantially between cycles, except for the top layer between cycles 3 and 4 at the 24-hr measurement. The resistivity measurements for the top layer, cycles 1 to 4, were 1012, 1859, 2798, and 2664 ohm-cm at 24 hr. The resistivity measurements for the middle layer, cycles 1 to 4, were 820, 1676, 2411, and 2573 ohm-cm at 24 hr. The resistivity measurements for the bottom layer, cycles 1 to 4, were 704, 1152, 1881, and 2124 ohm-cm at 24 hr. For all layers, the resistivity increased with the number of cycles.

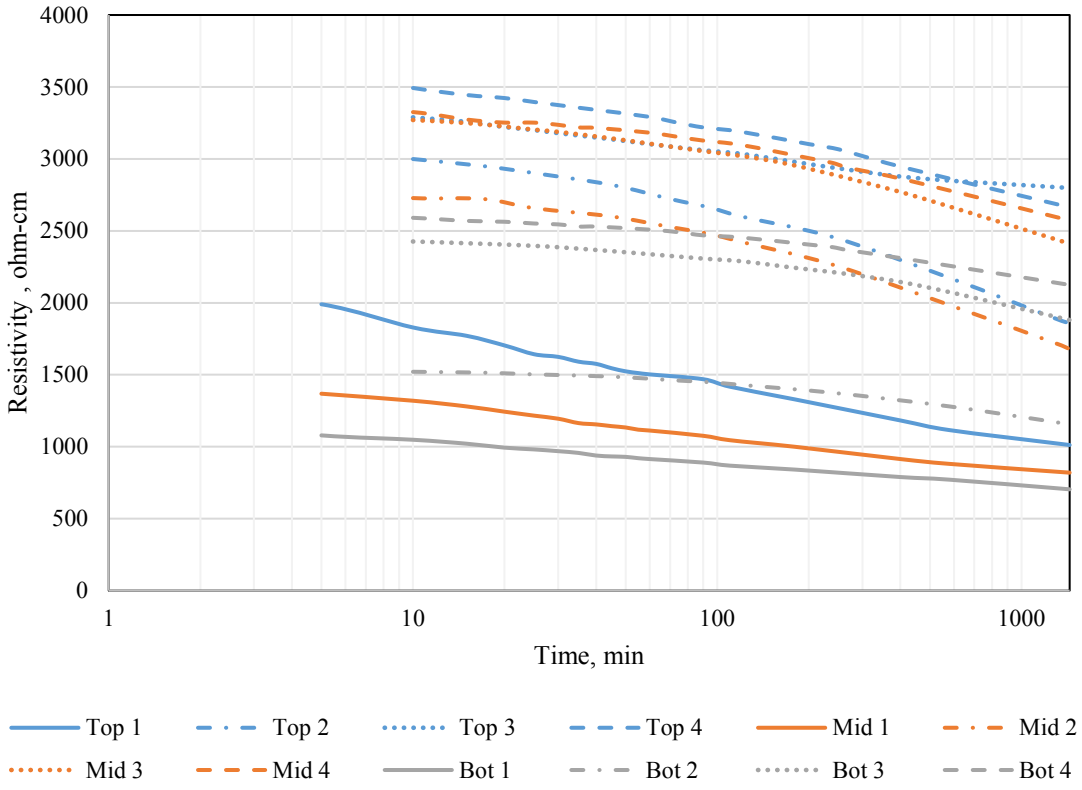

Figure 4.3.3a: Saturated Suffusion Box Resistivity Measurements on Material 3

Figure 4.3.3.b contains the drained resistivity measurements. As with Materials 1 and 2, resistivity values were very different depending on the elevation within the fill. Resistivity values were much higher for the middle and upper portions of the sample and increased with each cycle until the reading was out of range. Resistivity for the bottom layer also increased with the number of cycles, but to a much lesser degree, and resistivity declined somewhat during each cycle. For the top layer, the first cycle reached the maximum measurement at 440 min. For Cycle 2 the top layer reached the maximum at 40 min, and for cycles 3 and 4, the top layer was above the 2000-ohm maximum at the initial measurement. For the bottom layer, the resistivity values for cycles 1 to 4 were 3548, 5121, 6614, and 8199 ohm-cm.

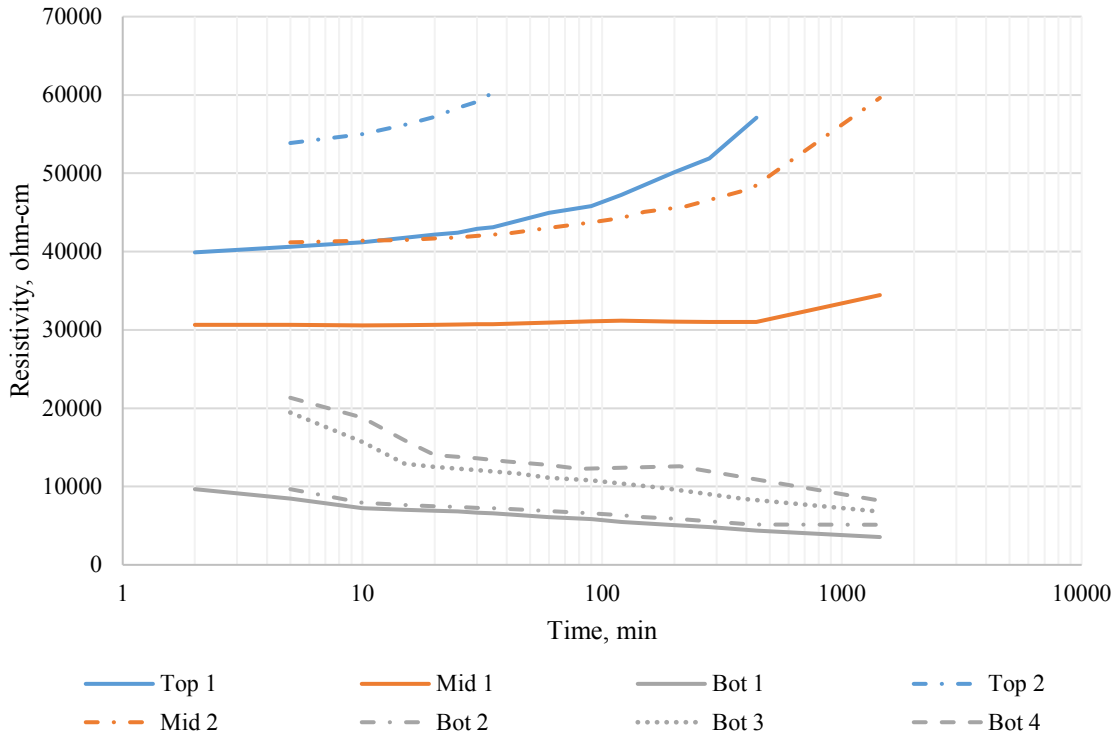

Figure 4.3.3b: Drained Suffusion Box Resistivity Measurements on Material 3

4.3.4 Test 4 Material

The material tested was collected from Wichita, Kansas. Figure 4.3.4a shows the saturated resistivity measurements. Resistivity values were largely stable, with steady, small declines occurring over the 24-hr cycles for most cases. Resistivity values increased substantially with each cycle. The resistivity measurements for the top pair of plates for Cycles 1 to 4 were 1326, 5069, 4587, and 4511 ohm-cm at 24 hr. The resistivity measurements for the middle pair for Cycles 1 to 4 were 1113, 3036, 4962, and 6248 ohm-cm at 24 hr. The resistivity measurements for the bottom pair for Cycles 1 to 4 were 945, 1487, 3014, and 4337 ohm-cm at 24 hr. For the top pair, Cycle 2 at 420 min began to experience an increase in resistivity from ~4000 to ~5000 ohm-cm over a period of 1000 min. This behavior was not observed in Cycles 1, 3, or 4. In addition, readings for the top pair for Cycles 3 and 4 follow a nearly identical trend of resistivity measurements over 24 hr, and their lines intersect at several positions.

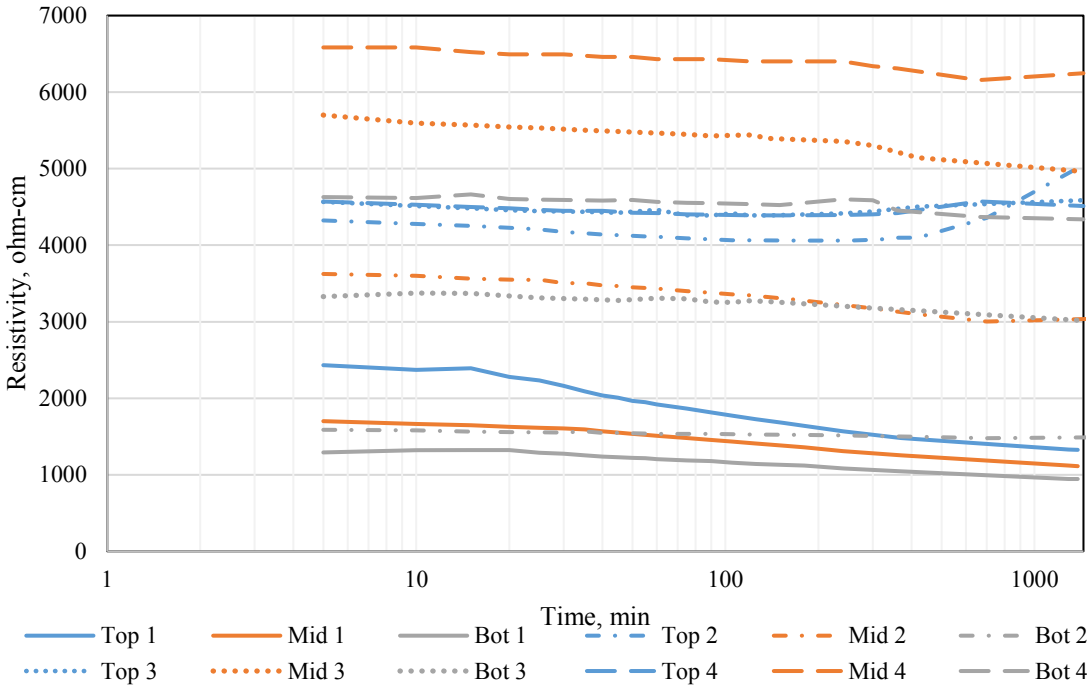

Figure 4.3.4a: Saturated Suffusion Box Resistivity Measurements on Material 4

Figure 4.3.4b contains the drained resistivity measurements. As with the previous materials, drained resistivity increased substantially with cycling of water, and the resistivity of the upper and lower portions of the backfill were substantially different. The resistivity at 24 hr for the top for Cycle 1 was 45,500 ohm-cm. The middle resistivity measurements at 24 hr for Cycles 1 to 3 were 16,642, 42,367, and 59,040 for 24 hr; and for Cycle 4, 60,503 ohm-cm for 90 min. The bottom resistivity measurements at 24 hr for Cycles 1 to 4 were 2067, 3658, 8839, and 12,497 ohm-cm.

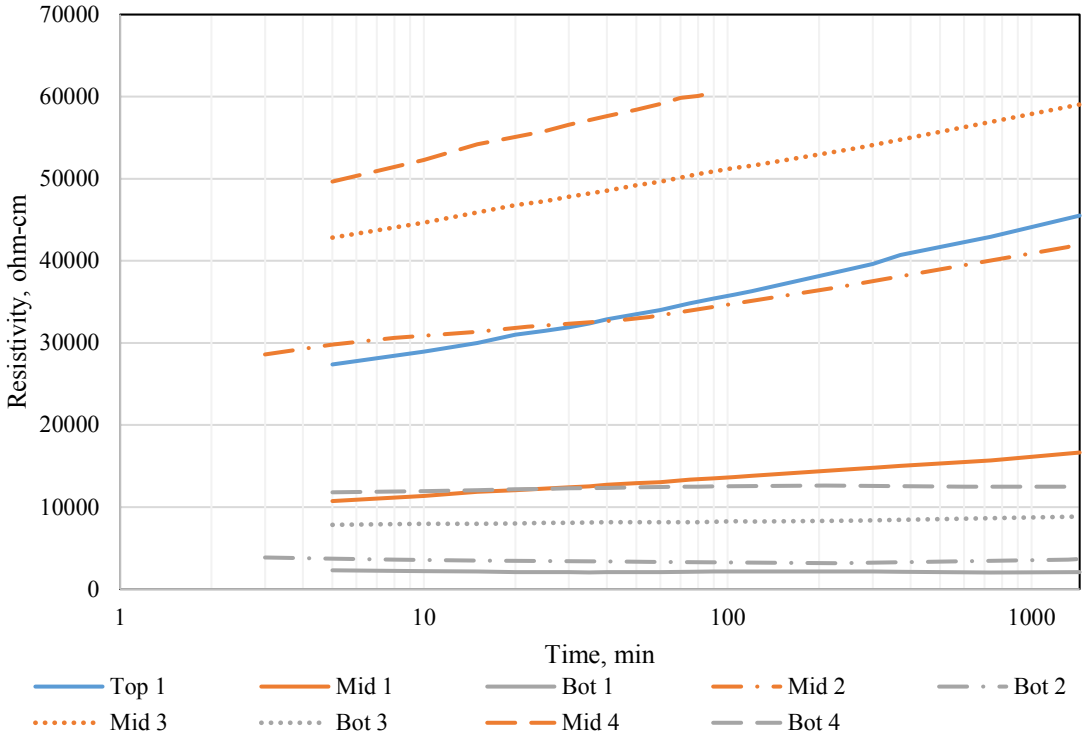

Figure 4.3.4b: Drained Suffusion Box Resistivity Measurements on Material 4

4.3.5 Test 5 Material

Test 5 material was from Wichita, Kansas. Test 5 material was the only sand aggregate tested. Figure 4.3.5a shows the measured results for the saturated cycles for the material.

Resistivity values were very stable during each cycle in most cases. Cycle 1 for the top layer was an exception. A substantial resistivity "dip" occurred during the first 500 min of this cycle. This was a result of the box cracking and creating a leak that only affected the top layer, as the bottom two layers were able to remain saturated for the entirety of the test. The leak was fixed, but DI water had to be continuously added to the top of the box. This resulted in the trend shown in Figure 4.3.5a. After 500 min the leak was fixed and the resistivity measurements returned to near the original value. As Figure 4.3.5a shows, the results for the top layer at 24 hr for cycles 1 to 4 were 10,668, 13,137, 9,754, and 10,363 ohm-cm. The results for the middle layer at 24 hr for cycles 1 to 4 were 9906, 14,417, 9601, and 9936 ohm-cm. The results for the bottom layer at 24 hr for cycles 1 to 4 were 9357, 11,918, 9205, and 8047 ohm-cm. For the sand, Cycle 2 had the higher resistivity measurements than cycle 4, which is not expected considering the other trends.

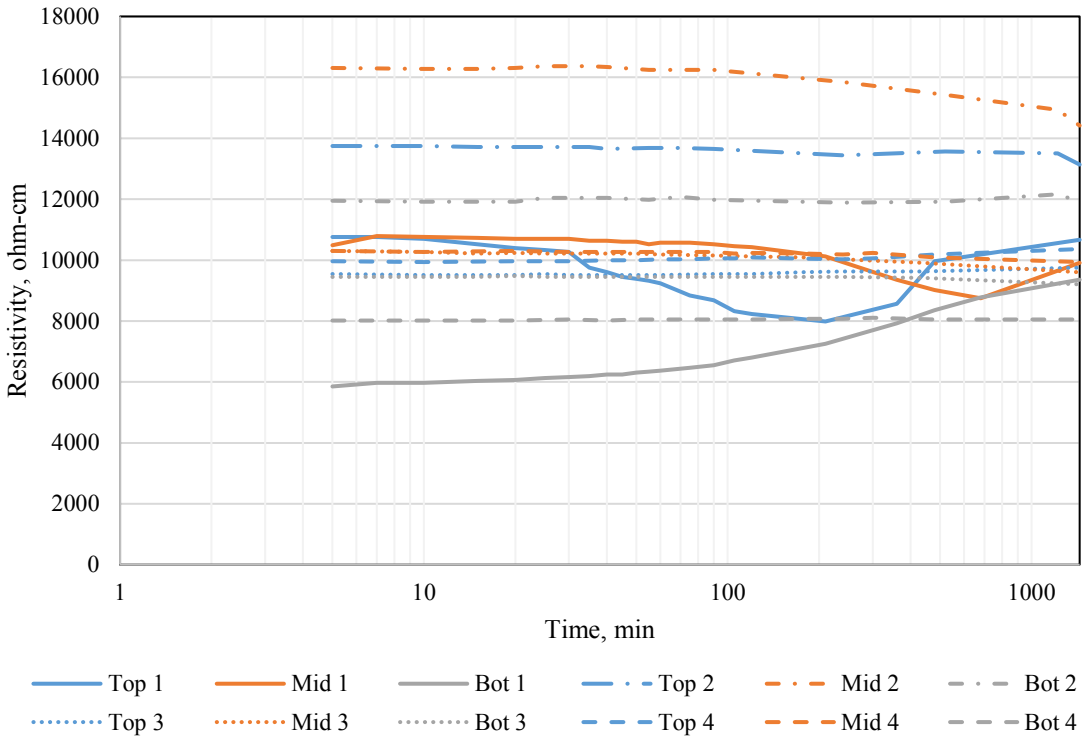

Figure 4.3.5a: Saturated Suffusion Box Resistivity Measurements on Material 5

Figure 4.3.5b contains the measured resistivity values for the drained cycles within the Suffusion Box. Resistivity values increased during each cycle for all elevations during all cycles except for the bottom layer during Cycle 1. Resistivity values were much higher for the top and middle portions of the fill than the bottom of the fill, to the point that resistivity could not be measured for any cycles for the top and middle layers after draining for 24 hr. For the top layer during Drained Cycle 1, at 15 min the resistivity measured was 60,838 ohm-cm. For Drained Cycle 2 at 15 min, the resistivity measured was 56,449 ohm-cm. For Drained Cycle 3 at 5 min, the resistivity was 53,645 ohm-cm, and for Cycle 4 at 15 min, the resistivity was 60,168 ohm-cm. For the middle layer for Cycles 1 through 4, the resistivity measurements were 60,168 ohm-cm at 50 min; 60,076 ohm-cm at 100 min; 59,985 ohm-cm at 150 min; and 48,890 ohm-cm at 75 min. For the bottom layer at 24 hr for Cycles 1 to 4, the resistivity measurements were much lower at 13,045, 17,400, 16,434, and 14,885 ohm-cm.

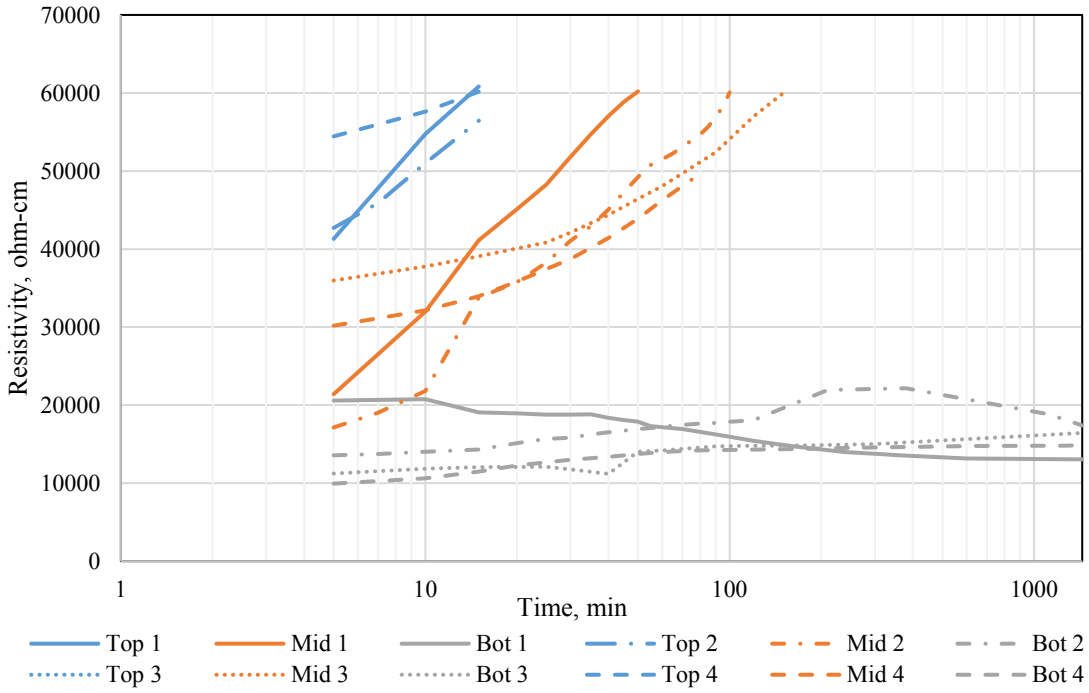

Figure 4.3.5b: Drained Suffusion Box Resistivity Measurements on Material 5

CHAPTER 5: DISCUSSION

5.1 Grain Size Distribution and Moisture Content

Based on KDOT Section 1107, "Aggregates for Backfill," the five materials tested passed the criteria from Table 4.1. With regard to resistivity testing, Brady et al. (2016) stated, "testing material passing the No. 10 (2 mm diameter) sieve would be unrepresentative as the mineralogy of the material may differ and may bias the sample." For example, a limestone member embedded with clay layers will have different percentages of minerals when passed through larger sieves compared to the material passing smaller sieves. As a result, a goal of this research was to test the full particle range within the aggregate to obtain a more representative resistivity measurement that would better replicate field conditions.

When comparing the percentages of material passing the No. 40 to 200 sieves for Materials 1 through 4 (the four larger aggregate backfills), Louisburg had the highest percentage passing, Kansas City was second, DeSoto was third, and Olathe had the lowest. Comparing the quarry tests with KU lab tests for gradation, Materials 1 and 3 gave a finer gradation closer to the lower limits put in place by KDOT, as shown in Figures 4.1.1a and 4.1.3a.

For Materials 2 and 4, the KU lab gradation gave a coarser gradation than quarry tests, as shown in Figures 4.1.2a and 4.1.4a. For Material 5, similar gradations were found in the quarry tests and KU lab tests. Quarry tests provide a more representative distribution, as the sample size is larger than in lab sample size guided by ASTM C136, *Sieve Analysis of Fine and Coarse Aggregates.* The discrepancy between quarry and KU lab gradation is likely due to natural sample variation.

Table 5.1: Percent Passing the No. 200 Sieve for Each Layer within Suffusion Box

	Percent Passing No. 200, Fine Material				
	Material 1	**Material 2**	**Material 3**	**Material 4**	**Material 5**
Top	1.3%	0.9%	0.3%	3.0%	0.42%
Middle	1.9%	1.2%	0.5%	3.1%	0.33%
Bottom	2.9%	1.9%	1.6%	5.3%	0.37%

Table 5.2: Moisture Content within Suffusion Box

	Moisture Content				
	Material 1	**Material 2**	**Material 3**	**Material 4**	**Material 5**
Top	5.4%	4.8%	3.7%	4.9%	2.0%
Middle	--	5.9%	4.4%	4.9%	2.4%
Bottom	7.7%	6.8%	5.2%	5.9%	10.7%

Tables 5.1 and 5.2 give the data collected within the Suffusion Box after the saturation and drainage cycles were completed. The tables show that for Materials 1 to 4, as there is an increase in fines, the moisture content also increases. The water flows downward during drainage, so the bottom layer is expected to have more fines as well as more water near the drainage hole. The water content was lowest in the top layer and highest in bottom layer for all five aggregates. As shown in Figure 5.1, the trend for Material 1 through 4 was an increase in fines and the moisture content. Material 5, the sand, did not show the same trend.

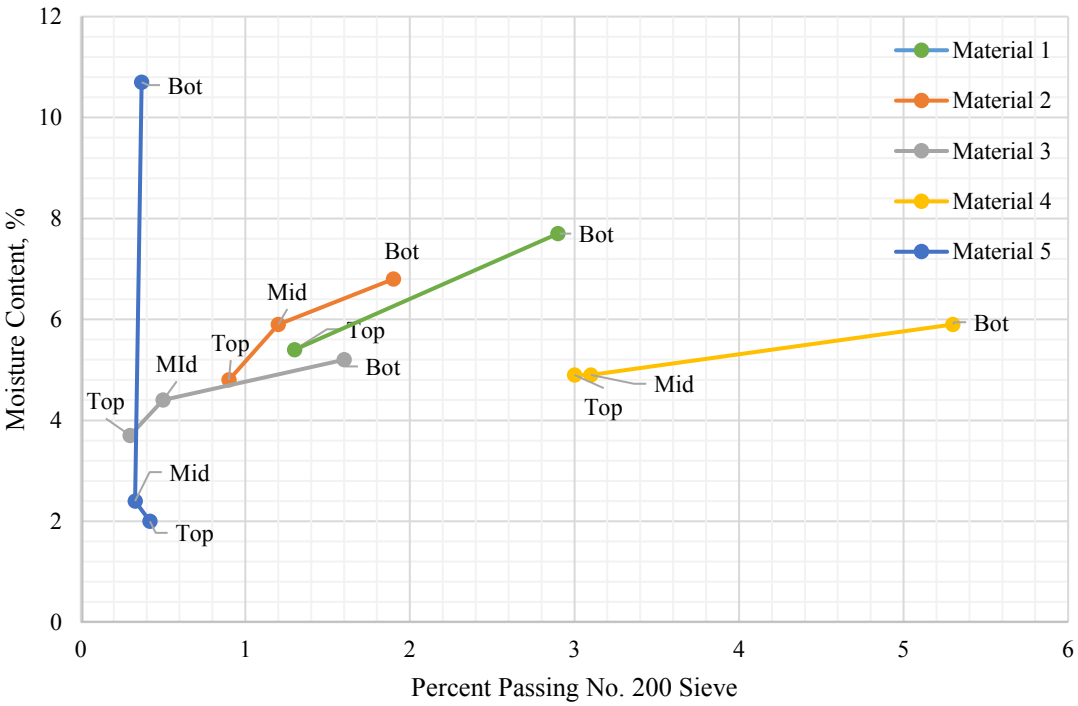

Figure 5.1: Moisture Content versus Percent Passing No. 200 Sieve

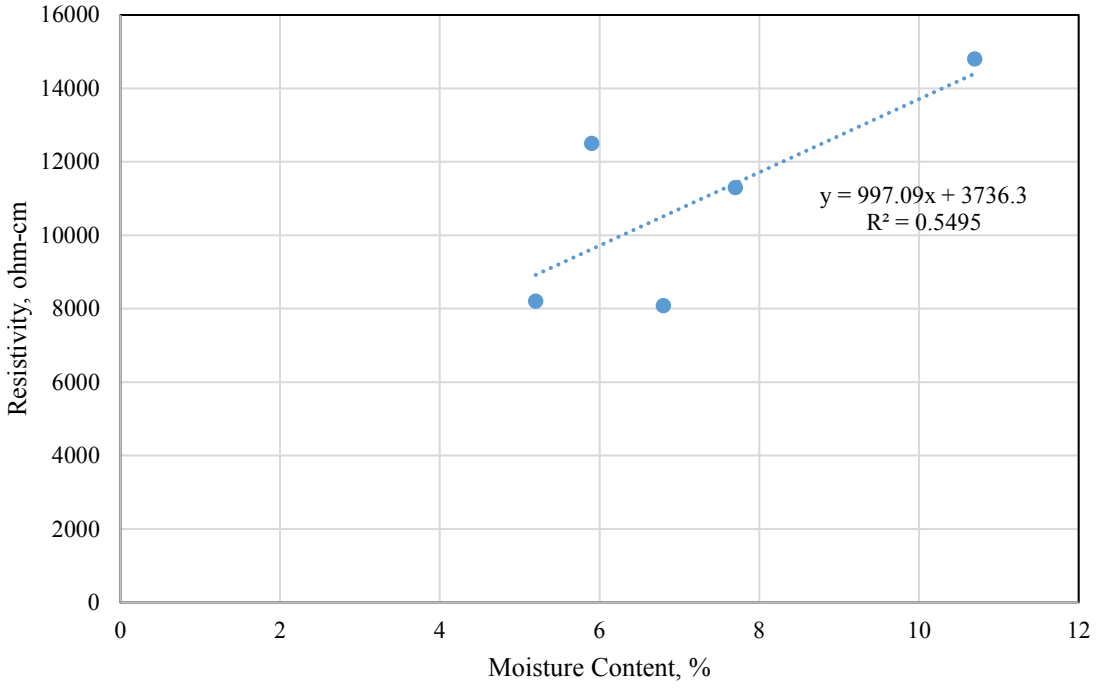

Figure 5.2: Resistivity versus Moisture Content

Figure 5.2 shows the general trend: as moisture content increases, the resistivity increases. The moisture content and resistivity values are from the final drained condition within the Suffusion Box for the bottom layer, as the data was only available for collection at the end the test once the Suffusion Box was opened.

5.2 SUFFUSION

A similar trend was observed for the top, middle, and bottom sections in all aggregate gradations after testing within the Suffusion Box. The bottom always had a higher percentage of fines compared to the top portion of the Suffusion Box. This was caused by the internal erosion, commonly called suffusion, which is due to water migrating downward during the filling and draining processes. This can be seen via video and images for the first four aggregate samples where finer material is transported through the voids within the larger aggregate. Examples are shown in Figure 5.3 for Test Materials 2 and 4 during the drainage cycles. Finer material can be seen migrating within the water as it is transported through the voids downward in the test column within the Suffusion Box.

Figure 5.3: Close-Up of Coarse Aggregate with Fines Transported During a Drainage Cycle

Correlations between the percentage passing the smaller sieves with the resistivity measurements are made in Section 5.3.

5.3 NEMA Box Resistivity

The NEMA Box was used for conventional resistivity testing of all aggregates examined in this study in accordance with the proposed ASTM protocol. For Materials 1 and 2, only the saturated cycle resistivity tests were recorded, because the drained cycles exceeded the 2000-ohm limit for the AEMC device. For Materials 3 to 5, the saturated and drained resistivity measurements were recorded. For Materials 1 to 5, a common trend for resistivity measurements was observed. As the number of saturated cycles increased, the resistivity increased. This is likely due to flushing

of ions from the sample and potentially some fines loss. In addition, for saturated cycles, Figures 4.2.1a to 4.2.5a show that after the first 400 to 500 min the resistivity trend would plateau or have a linear slope to the 24-hr mark.

Based on resistivity measurements from Materials 1 and 4, the resistivity was lower for saturated conditions than drained conditions. For Materials 1 and 2 the resistivity for the drained condition exceeded the upper limit of the AEMC device, and for Materials 3 and 4 the resistivity measurements for the drained condition were two to three times the reading for the saturated conditions. Also, as the number of drained cycles increased, the resistivity increased until the resistance was beyond the measurement limit of the AEMC instrument. For Material 3, Drained Cycles 2 and 3, the maximum resistance measurement for the AEMC device was exceeded during the first cycle before the 24-hr limit was reached. The AEMC instrument limit was not exceeded for Materials 4 and 5, even after all four drained cycles reached the 24-hr measurement. Figure 4.2.5a and b show that, for Material 5, the magnitude of the increase between saturated and drained conditions is less than for Materials 1 and 4. This is likely due to the fact that sand did not have many fines leave the system during the draining process, and the amount of water left within the sand during draining was greater due to the capillary pressure causing more water to remain within the NEMA Box. The increase in resistivity with the number of cycles is likely due to ions in the pore water and some fines leaving the box system during the drained cycles.

5.4 SUFFUSION BOX RESISTIVITY

The overall resistivity trends within the Suffusion Box were similar to those observed in the NEMA Box. As the number of cycles of pore fluid increased, the resistivity increased. This can be seen in the data for the saturated and drained cycles shown within the Suffusion Box results

section. Two examples can be seen in Figures 4.3.1a and 4.3.2a alongside with Figures 4.3.1b and 4.3.2b, which the saturated and drained resistivity increased with the number of cycles.

As described in the previous section, this increase in resistivity is likely due to the washing out of pore fluid with a high ion content and some fines loss. However, unlike the NEMA Box, the Suffusion Box has three pairs of electrodes for measuring resistivity at the top, middle, and bottom sections. In all cases, the bottom set of electrodes measured a lower resistivity than the top. This was attributed to the internal suffusion of fines and greater moisture retention. As shown in Figure 5.4, initially during the DI water filling phase for the first saturation cycles, fines were seen migrating downward with the DI water, causing the initial difference in resistivity for top, middle, and bottom layers. Figure 5.4 is a visual representation of the effect of the suffusion process after completion of the saturated and drained cycles for Materials 1, 2, and 4. Judging from Figure 5.3 and similar images for all for the aggregates, and from inspection during the filling and draining of the DI water, fines suffused downward in all cases, as shown in the gradation measurements comparing different layers. This led to dramatic differences in resistivity after draining based on elevation within the fill. Resistivity values in the upper and middle portions of the fill increased dramatically and usually exceeded the measurement capability of the AEMC instrument, while resistivity values at the base of the fill increased only modestly.

Though the resistivity increased each cycle, the magnitude of change per cycle for the saturated measurements was different than for the drained measurements. For instance, as shown in Figure 4.3.1a, the range in magnitude for saturated conditions between top and bottom resistivity measurements was less than 2000 ohm-cm, while for the drained cycle, as shown in Figure 4.3.1b, the range of resistivity measurements from top and bottom was 50,000 ohm-cm. This is similar to what was seen in other figures for the Suffusion Box. For the saturated case, it is likely the range

of resistivity was smaller as there was always pore water that provided the pathway for current. For the top layer of Materials 1 to 4 for the drained cases, a significant amount of fines migrated down through the aggregate with the water, and little pore water was held near the top of the fill, so fewer pathways remained for current to flow, leading to a higher resistivity. As mentioned in Section 5.1, the bottom layers for Materials 1 through 4 had more fine material. The higher fines content, enhanced by water draining downward, resulted in a layer with a higher moisture content compared to the other two layers. The increase in fines and higher moisture content for the bottom layer likely provided an increase in electrical pathways for current to travel, thus giving a lower resistivity measurement than for the top and middle layers.

Material 5 was the sand material from Wichita, Kansas. Compared to Materials 1 to 4, the sand (Material 5) did not have as much of an increase in fines for the bottom layer. This is based on the percentage increase of the No. 200 sieve for Materials 1 to 5 (223, 211, 482, 177, and 114%). Sand had the lowest increase in fines in the bottom of the Suffusion Box of the five materials.

Figure 5.4: Internal Erosion after Saturated and Drained Cycle Tests for Materials 1, 2, and 4 (left to right)

5.4.1 Finite Difference Modeling for Development of Resistivity Correction Factors

Resistivity is usually measured in the lab using a box (AASHTO T 288, ASTM CXXX-XX) that has known dimensions and two conductive plates mounted on opposite sides of the box that fully (or nearly fully) cover those sides of the box. The medium (soil) for which resistivity is to be measured is placed within the box, and a known current is passed between the two plates through the medium. By measuring the voltage required to transmit the current and using Ohm's Law (V = IR), the resistance is determined, and from that, the resistivity, as discussed in Chapter 2.

A fundamental assumption of this test procedure is that the current flow pathway is linear (see Figure 5.5). This is a good assumption for a box with regular dimensions and with plates on opposite sides of the box, where each plate fully covers its side of the box. This assumption is not well met with the Suffusion Box (Figure 5.6), where an individual plate covers less than 20% of one side. For this configuration, current flow will spread out to the additional medium volume above and below the elevations of the plates, and therefore a correction must be applied, or the current flow will be greater than expected and the calculated resistivity will be artificially low.

Correction factors were estimated using finite difference models of the Suffusion Box with the three plate sets activated. Electrical current flow can be modeled using the Laplace equation (Equation 5.1) in the same way as water flow using the finite difference method (for saturated conditions); therefore, an electrical current flow finite difference model was constructed where the following quantities are analogous.

$$\frac{\partial^2 h}{\partial x^2} + \frac{\partial^2 h}{\partial y^2} = 0 \qquad \textbf{Equation 5.1}$$

Equivalent quantities:

Flowrate (Q) = Current (I)

Total head (h) = Voltage (V)

Hydraulic Conductivity (K) = 1 / resistivity (1/ρ)

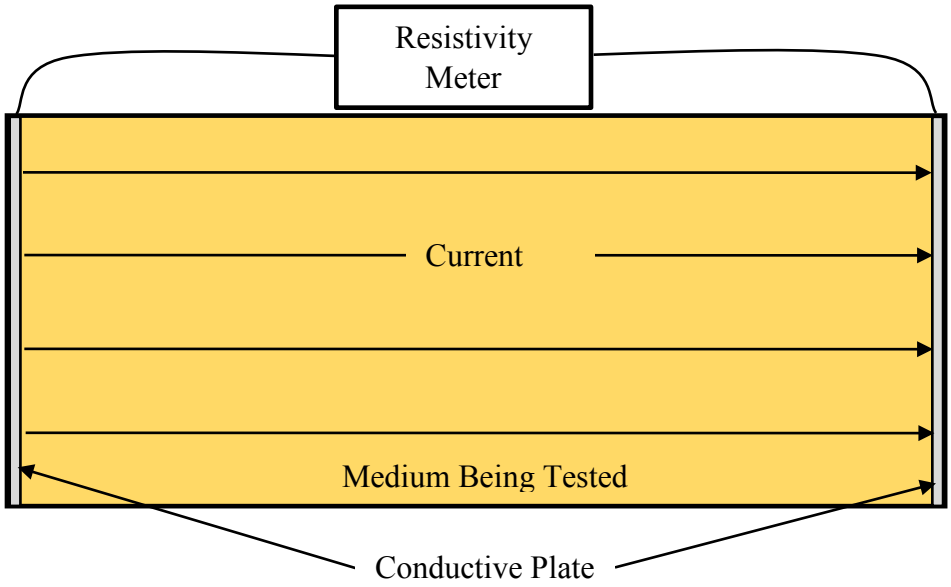

Figure 5.5: Standard Resistivity Box Configuration

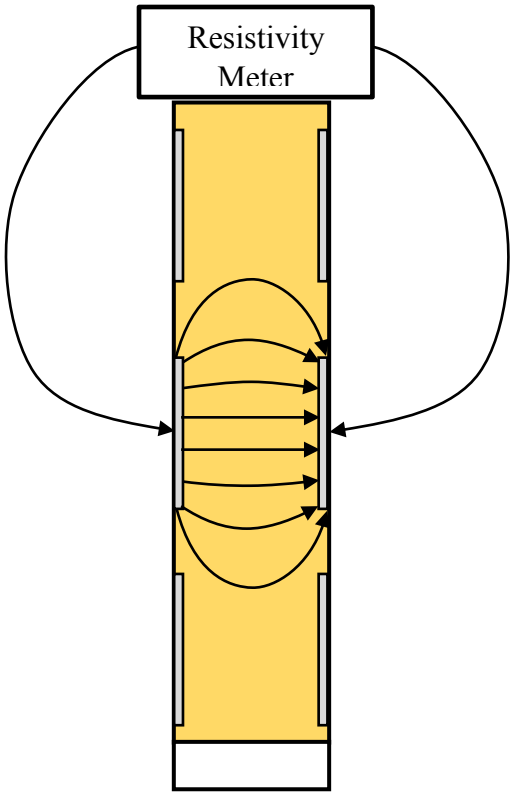

Figure 5.6: Conceptual Current Flow Path for Suffusion Box with Middle Plates Activated

For a system modeled as a set of nodes aligned in a series of rows and columns with uniform spacing (Δx = Δy), the value of total head (or voltage) at node location (i, j) can be approximated by substituting the terms in Equations 5.2 and 5.3 into the Laplace equation, Equation 5.4.

$$\frac{\partial^2 h}{\partial x^2} \approx \frac{h_{i+1}+2h_i+h_{i-1}}{(\Delta x)^2} \qquad \textbf{Equation 5.2}$$

$$\frac{\partial^2 h}{\partial y^2} \approx \frac{h_{j+1}+2h_j+h_{j-1}}{(\Delta y)^2} \qquad \textbf{Equation 5.3}$$

$$\frac{\partial^2 h}{\partial x^2} + \frac{\partial^2 h}{\partial y^2} \approx \frac{h_{i+1}+2h_i+h_{i-1}}{(\Delta x)^2} + \frac{h_{j+1}+2h_j+h_{j-1}}{(\Delta y)^2} = 0 \qquad \textbf{Equation 5.4}$$

Equation 5.4 can then be reduced to Equation 5.5. Equation 5.5 is then used to calculate the head (potential) values at all locations within the model, except for boundary nodes, which have slightly modified formulas. Values are then computed using the Gauss-Seidel iteration until they sufficiently converge. More detailed discussions and examples of finite difference modeling of groundwater flow are presented by Wang and Anderson (1982) and Bardet (1997).

$$h_{i,j} = \frac{h_{i+1} + h_{i-1} + h_{j+1} + h_{j-1}}{4} \qquad \textbf{Equation 5.5}$$

A 2-D finite difference reference model was constructed for the volume directly between the Suffusion Box plates to represent a theoretical box with a height that matched the Suffusion Box plate height and with the same width as the Suffusion Box. This theoretical box was used to calculate the box factor reported in Table 3.3. Nodes were established on a 1-cm spacing and distances were rounded to the nearest centimeter. The length (third dimension) was 30.5 cm; however, a unit thickness of 1 cm was used for the 2-D model, resulting in model dimensions of 30 by 30 by 1 cm. Using reference values of K = 1 cm/s, a head (potential) difference of 100 cm, and a unit thickness of 1 cm, a reference value for Q of 100 $cm^3/s/cm$ was determined. The reference model is shown in Figure 5.7. This system has constant area and constant velocity, so Q can be calculated directly from the formula for flow, Q = KiA, where i is the hydraulic gradient and A is the cross-sectional area. As shown in Equation 5.6, use of this formula yields a Q of 100 $cm^3/s/cm$.

$$Q = KiA = \left(1\frac{cm}{s}\right)\left(\frac{100cm}{30cm}\right)(30cm * 1) = 100\frac{cm^3}{s * cm} \qquad \textbf{Equation 5.6}$$

	0	1	2	3	4	5	6	7	8	9	10	11	12	13	14	15	16	17	18	19	20	21	22	23	24	25	26	27	28	29	30	31
30	100	97	94	90	87	84	81	77	74	71	68	65	61	58	55	52	48	45	42	39	35	32	29	26	23	19	16	13	10	6	3	0
29	100	97	94	90	87	84	81	77	74	71	68	65	61	58	55	52	48	45	42	39	35	32	29	26	23	19	16	13	10	6	3	0
28	100	97	94	90	87	84	81	77	74	71	68	65	61	58	55	52	48	45	42	39	35	32	29	26	23	19	16	13	10	6	3	0
27	100	97	94	90	87	84	81	77	74	71	68	65	61	58	55	52	48	45	42	39	35	32	29	26	23	19	16	13	10	6	3	0
26	100	97	94	90	87	84	81	77	74	71	68	65	61	58	55	52	48	45	42	39	35	32	29	26	23	19	16	13	10	6	3	0
25	100	97	94	90	87	84	81	77	74	71	68	65	61	58	55	52	48	45	42	39	35	32	29	26	23	19	16	13	10	6	3	0
24	100	97	94	90	87	84	81	77	74	71	68	65	61	58	55	52	48	45	42	39	35	32	29	26	23	19	16	13	10	6	3	0
23	100	97	94	90	87	84	81	77	74	71	68	65	61	58	55	52	48	45	42	39	35	32	29	26	23	19	16	13	10	6	3	0
22	100	97	94	90	87	84	81	77	74	71	68	65	61	58	55	52	48	45	42	39	35	32	29	26	23	19	16	13	10	6	3	0
21	100	97	94	90	87	84	81	77	74	71	68	65	61	58	55	52	48	45	42	39	35	32	29	26	23	19	16	13	10	6	3	0
20	100	97	94	90	87	84	81	77	74	71	68	65	61	58	55	52	48	45	42	39	35	32	29	26	23	19	16	13	10	6	3	0
19	100	97	94	90	87	84	81	77	74	71	68	65	61	58	55	52	48	45	42	39	35	32	29	26	23	19	16	13	10	6	3	0
18	100	97	94	90	87	84	81	77	74	71	68	65	61	58	55	52	48	45	42	39	35	32	29	26	23	19	16	13	10	6	3	0
17	100	97	94	90	87	84	81	77	74	71	68	65	61	58	55	52	48	45	42	39	35	32	29	26	23	19	16	13	10	6	3	0
16	100	97	94	90	87	84	81	77	74	71	68	65	61	58	55	52	48	45	42	39	35	32	29	26	23	19	16	13	10	6	3	0
15	100	97	94	90	87	84	81	77	74	71	68	65	61	58	55	52	48	45	42	39	35	32	29	26	23	19	16	13	10	6	3	0
14	100	97	94	90	87	84	81	77	74	71	68	65	61	58	55	52	48	45	42	39	35	32	29	26	23	19	16	13	10	6	3	0
13	100	97	94	90	87	84	81	77	74	71	68	65	61	58	55	52	48	45	42	39	35	32	29	26	23	19	16	13	10	6	3	0
12	100	97	94	90	87	84	81	77	74	71	68	65	61	58	55	52	48	45	42	39	35	32	29	26	23	19	16	13	10	6	3	0
11	100	97	94	90	87	84	81	77	74	71	68	65	61	58	55	52	48	45	42	39	35	32	29	26	23	19	16	13	10	6	3	0
10	100	97	94	90	87	84	81	77	74	71	68	65	61	58	55	52	48	45	42	39	35	32	29	26	23	19	16	13	10	6	3	0
9	100	97	94	90	87	84	81	77	74	71	68	65	61	58	55	52	48	45	42	39	35	32	29	26	23	19	16	13	10	6	3	0
8	100	97	94	90	87	84	81	77	74	71	68	65	61	58	55	52	48	45	42	39	35	32	29	26	23	19	16	13	10	6	3	0
7	100	97	94	90	87	84	81	77	74	71	68	65	61	58	55	52	48	45	42	39	35	32	29	26	23	19	16	13	10	6	3	0
6	100	97	94	90	87	84	81	77	74	71	68	65	61	58	55	52	48	45	42	39	35	32	29	26	23	19	16	13	10	6	3	0
5	100	97	94	90	87	84	81	77	74	71	68	65	61	58	55	52	48	45	42	39	35	32	29	26	23	19	16	13	10	6	3	0
4	100	97	94	90	87	84	81	77	74	71	68	65	61	58	55	52	48	45	42	39	35	32	29	26	23	19	16	13	10	6	3	0
3	100	97	94	90	87	84	81	77	74	71	68	65	61	58	55	52	48	45	42	39	35	32	29	26	23	19	16	13	10	6	3	0
2	100	97	94	90	87	84	81	77	74	71	68	65	61	58	55	52	48	45	42	39	35	32	29	26	23	19	16	13	10	6	3	0
1	100	97	94	90	87	84	81	77	74	71	68	65	61	58	55	52	48	45	42	39	35	32	29	26	23	19	16	13	10	6	3	0
0	100	97	94	90	87	84	81	77	74	71	68	65	61	58	55	52	48	45	42	39	35	32	29	26	23	19	16	13	10	6	3	0

Figure 5.7: Finite Difference Model of Box with Dimensions Equal to Suffusion Box Plate Dimensions

Flowrate can be calculated making use of the finite difference model using the same equation by applying it to each row along a column that passes entirely through the model. The total flowrate is the sum of these individual flowrates. For the model shown in Figure 5.8, the total flowrate was 100 $cm^3/s/cm$, which matches the analytical model and confirms that the finite difference model was constructed accurately.

Similar models were constructed for the Suffusion Box with nodes on a 1-cm spacing. Reference values of K = 1 cm/s, a head difference of 100 cm, and a unit length (third dimension) of 1 cm was also used. These models are shown in Figure 5.8. The solid red and green strips on the boundaries represent active electrodes. Significant flow occurs in the areas with higher gradients, which are areas where color changes over short distances. Most of the flow occurs in the area between the electrodes, although there is some flow above and below electrode elevations.

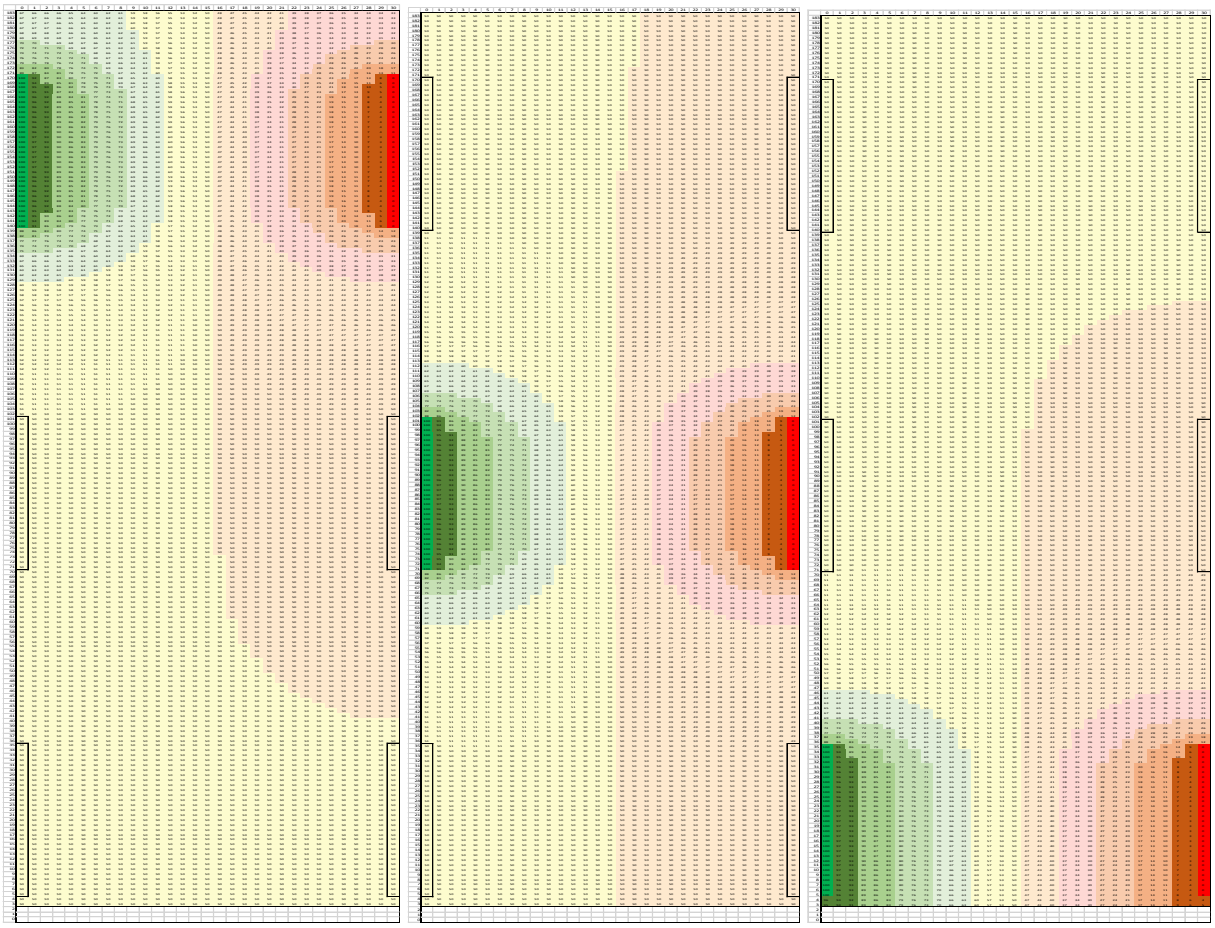

Figure 5.8: 2-D finite Difference Models for Suffusion Box Testing with Active Plate Pairs at the Top, Middle and Bottom of the Suffusion Box. Left = Top Pair activated. Center = Middle Pair. Right = Bottom Pair.

Unit flowrates for the three Suffusion Box configurations were computed and are shown in Table 5.3 along with the flowrate for the reference box. As Table 5.3 shows, flowrates were higher for all Suffusion Box models when compared with the reference model. Flowrates are very similar for the top and bottom models as their electrode configurations are a near mirror image of each other, while the model with active middle electrodes has the greatest flow because flow can occur well above and below the electrode elevations. The column for hydraulic conductivity (K, which is analogous to the electrical conductivity, σ) represents the conductivity required to achieve the same amount of flow through the reference box as occurred through the Suffusion Box for that

electrode configuration. For example, K for the reference box would need to be 1.44 times the value of K for the Suffusion Box with active top electrodes for the same flowrate to occur. Resistivity is equal to 1/σ (or 1/K).

Table 5.3: Flowrates for SB Finite Difference Models

Active Electrodes	Q ($cm^3/s/cm$)	K	R = 1/K
Top	144.3	1.44	0.69
Middle	146.5	1.47	0.68
Bottom	129.5	1.29	0.77
Reference	100.0	1.00	1.00

5.4.1.1 Calculation of K, R and the Resistivity Correction Factor

A resistance meter works by sending a fixed amount of current through the medium of interest. Voltage (V) is adjusted until the current (I) is at the correct value, and resistance (R) is determined by Ohm's law where R = V/I.

Given that

$$I = \frac{V}{R}$$ **Equation 5.7**

and that

$$R = \frac{\rho L}{A}$$ **Equation 5.8**

current is inversely proportional to resistance (R) and resistivity (ρ). Therefore, if current is higher than expected, the calculated resistivity will be lower than expected. For the case of the Suffusion Box, the measured resistance values for the top, middle, and bottom pairs of electrodes will be 76, 68, and 76%, respectively, of the values that would be measured in the reference box. To correct

for this, measured resistances should be multiplied by the values in Column K in Table 5.3 (or divided by the percentages) to get a corrected measure of resistance and a more accurate value for resistivity.

5.4.1.2 Applicability of These Correction Factors

An assumption underlying these models and correction factors is that the medium has a uniform resistivity. This is approximately the case for the saturated Suffusion Box tests, but is not the case for the drained Suffusion Box tests, where resistivity was much higher in the top of the sample than the bottom of the sample. This change in resistivity will affect flow somewhat. For the case where the top plates are active, relatively more flow would occur outside of the plate area because the volume below the plates is more conductive. For the case where the bottom plates are active, relatively less flow would occur outside the plate area because the volume above is somewhat less conductive. These conditions would cause the correction factor for the top plates to be somewhat greater than 1.44 and the correction factor for the lower electrodes to be somewhat less than 1.29 (but still greater than 1.0). The effect of this would be to increase the resistivity for the top of the sample. The resistivity for the bottom of the sample would also be increased, but not to the same degree; therefore, the spread in resistivity values between the top and bottom of the sample would be increased somewhat. Given the magnitude of the correction factors (~1.3 to 1.4), the effect would likely be small.

Figures 5.8 through 5.12 are the saturated resistivity measurements with the correction factors from Table 5.3 applied.

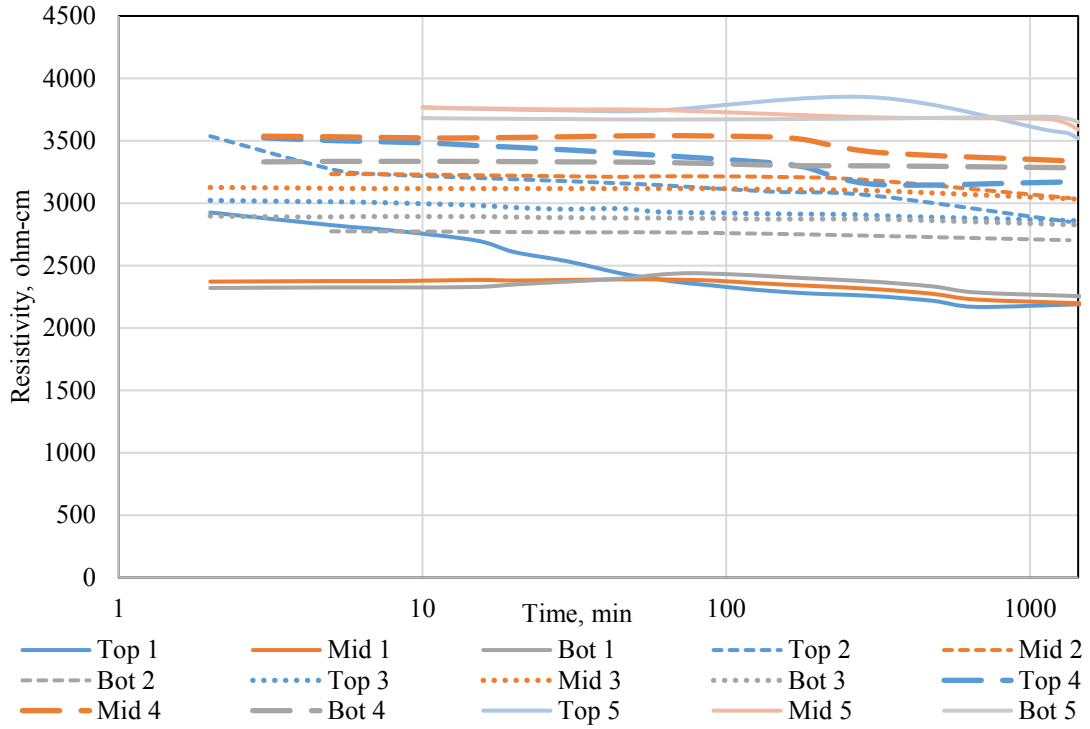

Figure 5.8: Corrected Saturated-Condition Resistivity Measurements for Suffusion Box Material 1

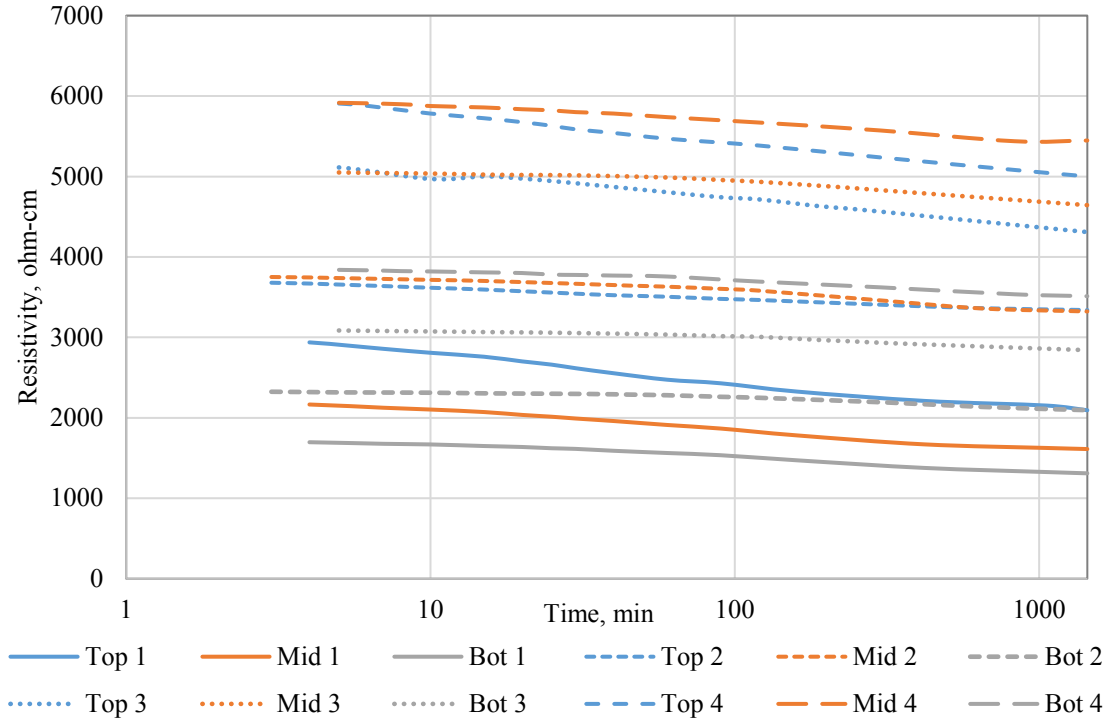

Figure 5.9: Corrected Saturated-Condition Resistivity Measurements for Suffusion Box Material 2

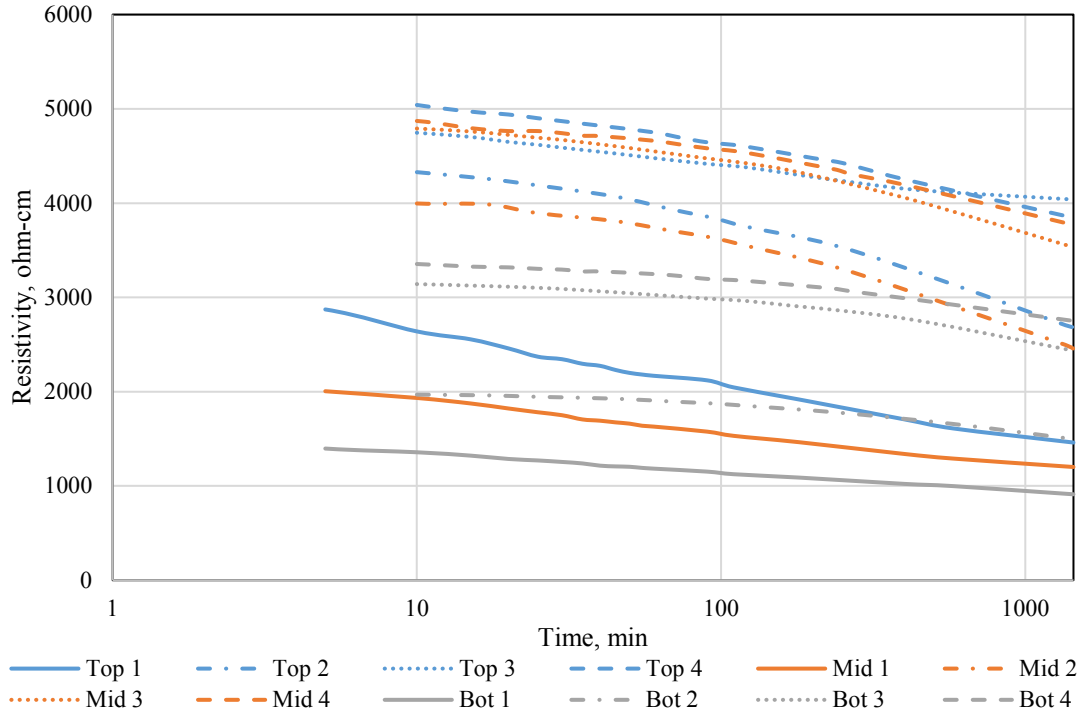

Figure 5.10: Corrected Saturated-Condition Resistivity Measurements for Suffusion Box Material 3

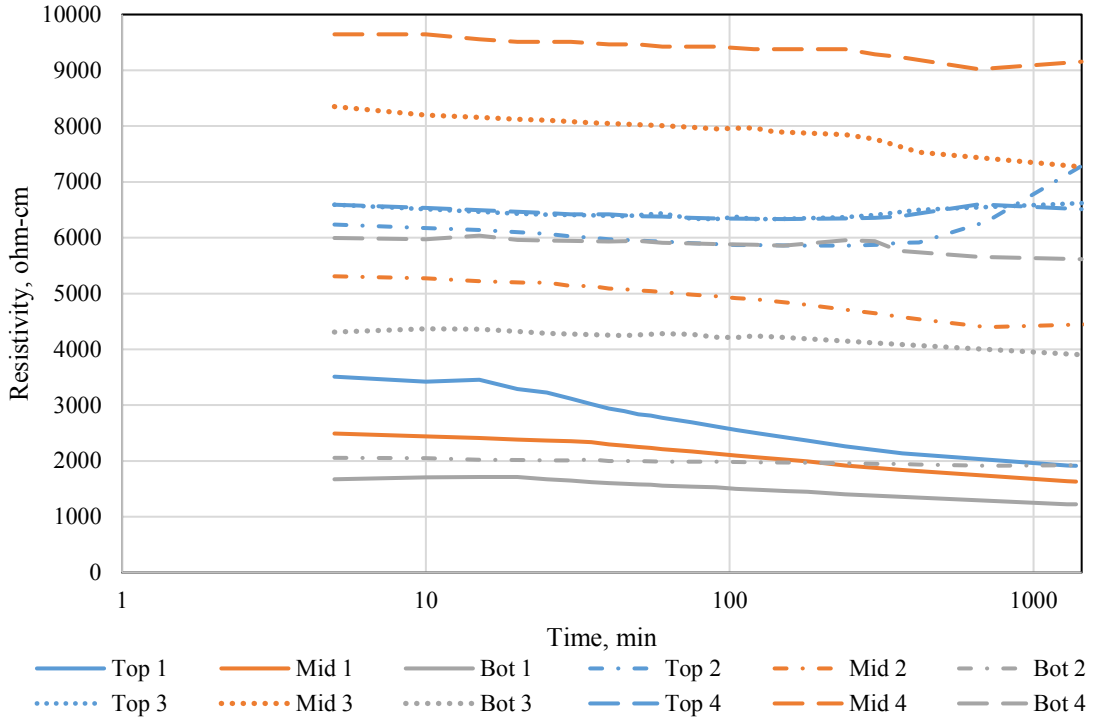

Figure 5.11: Corrected Saturated-Condition Resistivity Measurements for Suffusion Box Material 4

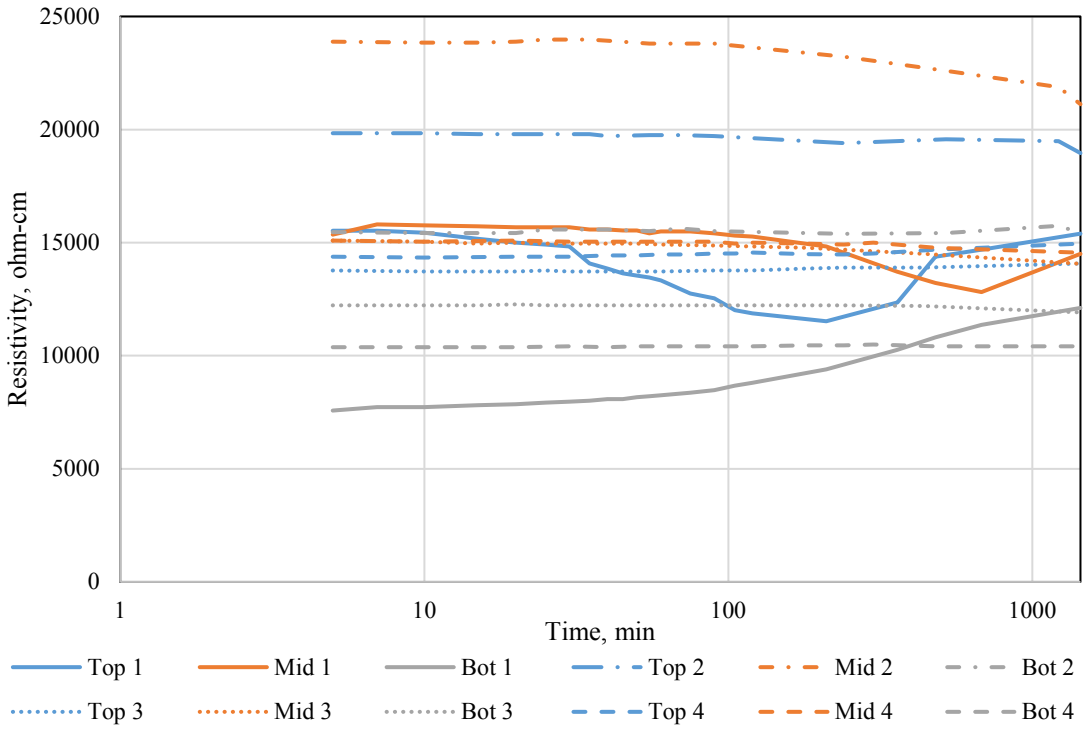

Figure 5.12: Corrected Saturated-Condition Resistivity Measurements for Suffusion Box Material 5

Table 5.4 NEMA and Suffusion Box Resistivity (ohm-cm) Comparison Table

	Material 1				Material 2			
	NEMA	Suffusion Box			NEMA	Suffusion Box		
	--	Top	Middle	Bottom	--	Top	Middle	Bottom
Saturated Cycle 1	2382	1518	1500	1740	2045	1430	1100	1012
Saturated Cycle 2	3363	1975	2076	2088	2473	2280	2268	1618
Saturated Cycle 3	4093	1981	2070	2182	3376	2941	3170	2195
Saturated Cycle 4	3735	2198	2277	2536	--	3414	3719	2713
Saturated Cycle 5	--	2438	2451	2819	--	--	--	--
Drained Cycle 1	> AEMC	> AEMC	40100	6217	> AEMC	> AEMC	33200	4054
Drained Cycle 2	> AEMC	> AEMC	50000	8047	> AEMC	> AEMC	> AEMC	6370
Drained Cycle 3	> AEMC	> AEMC	> AEMC	10300	> AEMC	> AEMC	> AEMC	6462
Drained Cycle 4	> AEMC	> AEMC	> AEMC	9693	> AEMC	> AEMC	> AEMC	8077
Drained Cycle 5	--	> AEMC	> AEMC	11300	> AEMC	--	--	--
	Material 3				Material 4			
	NEMA	Suffusion Box			NEMA	Suffusion Box		
	--	Top	Middle	Bottom	--	Top	Middle	Bottom
Saturated Cycle 1	1359	1012	820	704	2711	1326	1113	945
Saturated Cycle 2	2220	1859	1676	1152	5465	5069	3036	1487
Saturated Cycle 3	2977	2798	2411	1881	6499	4587	4962	3014
Saturated Cycle 4	--	2664	2573	2124	8398	4511	6248	4337
Saturated Cycle 5	--	--	--	--	--	--	--	--
Drained Cycle 1	21700	> AEMC	34400	3458	12766	45500	16600	2067
Drained Cycle 2	> AEMC	> AEMC	59600	5121	20151	> AEMC	42300	3658
Drained Cycle 3	> AEMC	> AEMC	> AEMC	6614	21142	> AEMC	59000	8839
Drained Cycle 4	> AEMC	> AEMC	> AEMC	8199	30890	> AEMC	> AEMC	12500
Drained Cycle 5	--	--	--	--	--	--	--	--
	Material 5							
	NEMA	Suffusion Box						
	--	Top	Middle	Bottom				
Saturated Cycle 1	15276	10668	9906	9357				
Saturated Cycle 2	13251	13137	14417	11918				
Saturated Cycle 3	11668	9754	9601	9205				
Saturated Cycle 4	11922	10363	9936	8047				
Saturated Cycle 5	--	--	--	--				
Drained Cycle 1	17534	> AEMC	> AEMC	13045				
Drained Cycle 2	16247	> AEMC	> AEMC	17400				
Drained Cycle 3	12783	> AEMC	> AEMC	16434				
Drained Cycle 4	14559	> AEMC	> AEMC	14885				
Drained Cycle 5	--	--	--	--				

Table 5.4 contains the 24-hr-duration resistivity values with units as ohm-cm for the NEMA and Suffusion Box. The lines indicate that data is unavailable, and " > AEMC" indicates that resistance exceeded 2000 ohms for the device.

Table 5.5 NEMA and Suffusion Box Resistivity (ohm-cm) Comparison Table, with Corrected Values for Saturated Conditions within Suffusion Box

	Material 1				**Material 2**			
	NEMA	**Suffusion Box**			**NEMA**	**Suffusion Box**		
	--	**Top**	**Middle**	**Bottom**	**--**	**Top**	**Middle**	**Bottom**
Saturated Cycle 1	2382	2191	2197	2253	2045	2094	1612	1310
Saturated Cycle 2	3363	2850	3041	2703	2473	3340	3322	2095
Saturated Cycle 3	4093	2859	3032	2825	3376	4309	4644	2841
Saturated Cycle 4	3735	3172	3336	3283	--	5001	5448	3512
Saturated Cycle 5	--	3519	3590	3650	--	--	--	--
	Material 3				**Material 4**			
	NEMA	**Suffusion Box**			**NEMA**	**Suffusion Box**		
	--	**Top**	**Middle**	**Bottom**	**--**	**Top**	**Middle**	**Bottom**
Saturated Cycle 1	1359	1460	1201	912	2711	1914	1630	1223
Saturated Cycle 2	2220	2683	2456	1492	5465	7315	4447	1926
Saturated Cycle 3	2977	4038	3532	2435	6499	6620	7269	3903
Saturated Cycle 4	--	3845	3769	2750	8398	6510	9154	5615
Saturated Cycle 5	--	--	--	--	--	--	--	--
	Material 5							
	NEMA	**Suffusion Box**						
	--	**Top**	**Middle**	**Bottom**				
Saturated Cycle 1	15276	15396	14512	12115				
Saturated Cycle 2	13251	18959	21121	15429				
Saturated Cycle 3	11668	14076	14066	11917				
Saturated Cycle 4	11922	14956	14557	10418				
Saturated Cycle 5	--	--	--	--				

Table 5.5 contains the 24-hr-duration resistivity values with units as ohm-cm for the NEMA and Suffusion Box. Correction values developed using the finite difference models were applied to obtain the values reported in Table 5. The applied correction values used can be found in Table 5.3.

CHAPTER 6: CONCLUSIONS AND RECOMMENDATIONS

This thesis contains the results of research on the potential for fines within MSE backfill to migrate downwards within the fill. Such migration has the potential to inhibit drainage, lower resistivity, and promote corrosion of reinforcement elements in the lower portion of the fill. Based on the results of this research, the following conclusions and recommendations were developed.

6.1 CONCLUSIONS

6.1.1 Gradation and Specifications

All aggregates tested were well within KDOT Special Provision 1100 specifications. However, this specification is quite broad and relatively easy to meet, with the possible exception of the requirement that less than 5% of the material is allowed to pass the No. 200 sieve. This requirement appears to be important and beneficial. Fines contents in all samples tested were low, with a maximum observed fines content of 5% for Material 1. This low fines content was likely beneficial because it limited the fines available for suffusion (migration) and accumulation at lower elevations.

6.1.2 Moisture Content and Grain Size Distribution for Suffusion Box

The moisture content for all aggregates increased from top to bottom within the Suffusion Box. Over the course of the saturated and drainage cycles within the Suffusion Box, aggregates had a greater decrease in the percentage passing the No. 40 or smaller sieves for the top third than the percentage passing the bottom third, which was considered to be strong evidence for suffusion. In addition, for Materials 1 through 4 (the large aggregate materials), an increase in fines was observed within the bottom section.

6.1.3 New ASTM CXXX-XX with the NEMA Box

For Materials 1 to 4 the resistivity increased substantially as the number of cycles of saturation and drainage increased. This was attributed to the flushing of ions and very fine suspended particles out of the system. For all aggregates, resistivity values were well above the 3000/5000-ohm-cm limit for the drained case and were occasionally so high they could not be measured. The drained case was considered more critical by the research team, as it should be more representative of field conditions for most walls. Exceptions to this would include walls where submerged conditions are anticipated for some portion of the reinforcement. For such cases, the resistivity for saturated conditions is likely more critical.

For Materials 1 through 4, the initial saturated measurements for resistivity were below the limit of 3000/5000 ohm-cm. Only after several cycles did the material pass the limit, likely due to ions and fines leaving the system during the drainage process. For Material 5, the sand material, the overall resistivity measurements decreased somewhat from a fairly high level as the number of cycles increased. Resistivity values for the sand remained well above the 3000/5000-ohm-cm limit despite this decline.

Trends for Material 5 were different from the other four materials, as resistivity declined somewhat with additional cycles of saturation and drainage. Resistivity measurements for the sand were ~11,000 to ~15,000 ohm-cm for the saturated condition, which is well above the 3000/5000-ohm-cm limit, and were similar for the drained condition.

6.1.4 Suffusion Box

Resistivity values discussed in this section were determined using a non-standard resistivity measurement that likely yields resistivity measurements that are low because of the

geometry of the test box and electrodes. However, any bias should be consistent for each elevation; therefore, the numbers reported should be valid for comparison purposes. Correction factors were developed using finite difference modeling, as discussed in Chapter 5. These factors were modest and on the order of 1.4.

For the Suffusion Box, Materials 1 to 4 had an overall increase in resistivity as the number of cycles of saturation and drainage increased. This was observed for both drained and saturated measurements. For the drained case, this increase was very large for the upper and middle elevations within the backfill and was much more modest for the lower elevations within the backfill, resulting in sharply different measures of resistivity for the different elevations. This difference was attributed to downward suffusion of fines within the materials, which led to cleaner aggregates that retained less water for the upper elevations and some concentration of fines and greater water retention for the lower elevations. Resistivity values for the drained condition remained above the 3000/5000-ohm-cm limit for all aggregates. For Material 5 (sand), there was also a very large difference in resistivity between the middle and upper elevations and the lower elevations; however, these differences were apparent from the first cycle and did not change much for subsequent cycles. These differences were likely due to differences in water content and suffusion that occurred during the first saturation cycle.

The drained condition better simulates field conditions, as an MSE wall is generally not designed to have a saturated backfill behind the wall. For the Suffusion Box, the bottom layer for drained conditions for Materials 1 to 5 was always lower than the middle and top resistivity measurements by a factor of two to three. In addition, the bottom measurements for the drained condition changed less than the top and middle elevations with cycling.

6.2 RECOMMENDATIONS

All materials tested met the current KDOT specifications. However, the current specifications permit a very wide range of grain size distributions to be used. It is conceivable that a gap-graded aggregate with a substantial fine fraction could permit significantly more particle migration than was observed during this research project. Some narrowing of these specifications may be beneficial in preventing future suffusion problems. The current specification limiting the amount of material passing the No. 200 sieve to no more than 5% of the total is believed to be beneficial, and it should be retained because it limits the fines available for suffusion.

Based on the research conducted, it is recommended that future Suffusion Box tests be conducted with a single molded shape due to challenges water-proofing the edge-to-edge connections. In addition to a single molded shape, a refinement of aggregate compaction procedures so the aggregate within the box is densified in a manner that better replicates field conditions.

For most cases, testing under drained conditions is probably more appropriate than saturated conditions. Exceptions to this would include walls where submerged conditions are anticipated for some portion of the reinforcement. For such cases, the resistivity for saturated conditions is likely more critical.

Finally, this project was focused on flow in one dimension (vertical), while for actual walls there is a horizontal component to the flow as water moves to a drainage sheet or pipe. This horizontal flow could cause additional concentration of fines. A larger box with centralized drains to capture 2- or 3-dimensional drainage, more closely representing MSE drainage, would provide an even more realistic understanding of fines migration through the backfill. Further research into

parameters such as void ratio, porosity, water content, water constituents, addition of sulfate and chlorides (from fertilizers and road salts), and mineralogy is recommended to aid in appropriate selection of wall backfill.

REFERENCES

AASHTO T 27-14 (2014). *Standard method of test for sieve analysis of fine and coarse aggregates.* Washington, DC: American Association of State Highway and Transportation Officials.

Arciniega, J. L. (2017). Impact of grain size distribution on resistivity of mechanically stabilized earth wall backfill materials. In *TRB 96th Annual Meeting Compendium of Papers*. Washington, DC: Transportation Research Board.

ASTM D75 / D75M-14 (2014). *Standard practice for sampling aggregates.* West Conshohocken, PA: ASTM International. doi: 10.1520/D0075_D0075M-14.

Bardet, J. (1997). *Experimental Soil Mechanics.* Upper Saddle River, New Jersey: Prentice Hall.

Brady, Z., Parsons, R., & Han, J. (2016). *Testing aggregate backfill for corrosion potential* (Report No. K-TRAN: KU-15-5). Lawrence, KS: Kansas Department of Transportation, College of Engineering, University of Kansas.

Chang, D. S., & Zhang, L. M. (2011). A stress-controlled erosion apparatus for studying internal erosion in soils. *Geotechnical Testing Journal, 34*(6), 579–589.

Edlebeck, J. E., & Beske, B. (2014). Identifying and quantifying material properties that impact aggregate resistivity of electrical substation surface material. *IEE Transactions on Power Delivery, 29*(5), 2248–2253.

Elias, V., Fishman, K. L., Christopher, B. R., & Berg, R. R. (2009). *Corrosion/degradation of soil reinforcements for mechanically stabilized earth walls and reinforced soil slopes* (FHWA Publication No. FHWA-NHI-09-087). Washington, DC: Federal Highway Administration.

Gladstone, R. A., Anderson, P. L., Fishman, K. L., & Withiam, J. L. (2006). Durability of galvanized soil reinforcement: more than 30 years of experience with mechanically stabilized earth. *Transportation Research Record: Journal of the Transportation Research Board, 1975,* 49–59.

Kenny, T. C., and Lau, D. (1985). Internal stability of granular filters. *Canadian Geotechnical Journal, 22*(2), 215–225.

Kansas Department of Transportation. *Division 1100 Aggregates.* 2007.

Marot, D., Bendahmane, F., & Nguyen, H. H. (2012). Influence of angularity of coarse fraction grains on internal erosion process. *ICSE6-075*, 887–894.

Marot, D., Rochim, A., Nguyen, H. H., Bendahmane, F., & Sibille, L. (2016). Assessing the susceptibility of gap-graded soils to internal erosion: Proposition of a new experimental methodology. *Nat Hazards, 83,* 365–388.

Romanoff, M. (1957). *Underground corrosion* (National Bureau of Standards Circular 579). Washington, DC: Government Printing Office.

Sibille, L., Marot, D., & Sail, Y. (2015). A description of internal erosion by suffusion and induced settlements on cohesionless granular matter. *Acta Geotechnia, 10,* 735–748.

Thapalia, A., Borrok, D. M., Nazarian, S., & Garibay, J. (2011). Assessment of corrosion potential of coarse backfill aggregates for mechanically stabilized earth walls. *Transportation Research Record: Journal of the Transportation Research Board, 2253,* 63–72.

Wan, C. F., & Fell, R. (2008). Assessing the potential of internal instability and suffusion in embankment dams and their foundations. *Journal of Geotechnical and Geoenvironmental Engineering, 134(3),* 401–407.

Wang, H. F., and Anderson, M. P. (1982). *Introduction to groundwater modeling: Finite difference and finite element methods.* New York: W. H. Freeman and Co.

Yzenas, J. J., Jr. (2014). New test method of measurement of aggregate resistivity using the two-electrode soil box method (ASTM WK24621). Submitted to ASTM Subcommittee C-09.20, designation CXXX-XX.